SPAN ANALYSIS OF OPTICAL FIBER TRANSMISSION BASED ON WDM, DWDM AND DQPSK.

A Thesis

Submitted to the Department of Computer Science and Engineering

of

BRAC UNIVERSITY

BY

MD. HUMAYUN KABIR

Student ID: 06310046

&

MD. ASADUZZAMAN ALL FARUQ

Student ID: 05310050

MD. TANVIR REZA

Student ID: 05210035

In Partial Fulfillment of the

Requirements for the Degree

of

Bachelor of Science in Electronics and Communication Engineering

May 2008

BRAC UNIVERSITY

DECLARATION

We hereby declare that this thesis is based on the results found by our self. Materials of work found by other researcher are mentioned by reference. This thesis, neither in whole nor in part, has been previously submitted for any degree.

Signature of Supervisor

Signature of the Author

ACKNOWLEDGMENTS

The successful completion of this report has seen many helping hands, without which this would have not been possible. However, the space involved does not allow us to mention everybody individually. We would like to express our special thanks and sincere gratitude to Dr. Tarik A Chowdhury. We deeply appreciate his enthusiasm and guidance in preparing this report. While doing this report we really enjoyed the work and also identified a lot about the technologies that we are going to apply. We would like to thank him on behalf of the excellent guidance through valuable advice and support as well. We would like to thank BRAC authority for their library and Internet facilities from where we got enormous information. Special thanks to LN Binh and B. Laville who taught us how to implement our thesis work.

.

ABSTRACT:

Today's world depending on frequent data communication, optical fiber is the most frequent physical backbone to transferring carrier information and sometimes it is distorted, attenuated and losses of information. Span analysis is the calculation and verification of a fiber-optic system's operating characteristics. This includes items such as fiber routing, electronics, wavelengths, fiber type, and circuit length. Attenuation and nonlinear considerations are the key parameters for loss-budget analysis.

Demandable ultra-wideband transmission over the Internet, Transmission techniques is now measured to be very important. Hence, upgrading current RZ-10Gbps DWDM optical systems with 40 Gbps channels multiplexed with accessible traffic infrastructure we can enlarge the capacity to Terabit/s with minimum advancement tasks. We apply the DPQPSK transmission technique of single light wave channel over optical fiber communication systems. It has capability to double the bit-rate compared to usual OOK signaling techniques.

For simulation we apply the block sets of communication and signal processing of the Matlab ™ Simulink. A high-capacity 20 Gbps (2 * 10 Gbps) and 40 Gbps (40*10 Gbps) can be extended from 10Gb/s channels. Theoretical background of the design of the optical DQPSK system is given. Detailed operation and purpose of each component model and its outcomes in Simulink Block sets are explained. Future plane which support DWDM operation to allow Tbps transmission with N x 40 Gbps systems are also draw round.

TABLE OF CONTENTS

List of Table

List of Figure:

1 Preamble

The demand for increasing the transmission capacity of optical fiber transmission systems has encouraged many researchers and companies to explore cheaper, high bandwidth optical fiber system alternatives. A substantial amount of research has been pursued into developing high transmission rate systems which now extend into the Tbps region [3]. A large proportion of these investigations have focused on the design of optical systems as a whole. By this we imply that many proposals made implement different performance improvement techniques such as the application of pre-transmission dispersion management, amplification and on some circumstances, investigate the benefits of utilizing different optical carrier sources [4].

An area of development which has had a great deal of research attention and applications is the dense wavelength division multiplexing (DWDM) optical fiber system. This system typically transmits multiple wavelengths on a single SM fiber. This method has been one of the key contributors to enhance the optical transmission channel capacity.

This report investigates the limitations of a single channel driven by the DQPSK signaling technique. Recently, interests have been shown towards the development of DQPSK transmission systems. These systems have been shown to be more tolerant to the effects of chromatic dispersion and other non-linear effects compared to conventional OOK[5]. The DQPSK technique also doubles the spectral efficiency (b/s/Hz) by encoding two bits of data per symbol in a differential phase shift format.

The development and simulation of an optical DQPSK transmission link system using Matlab Simulink are described. The system is compared, to within certain limitations, with experimental results published papers [6]. We have, in particular, analyzed the impairments on system performance due to chromatic dispersion effects, self phase modulation (SPM), non-linear effects and receiver noise effects. In order to access these effects we have implemented these real performance degrading effects into the simulations based on theoretical knowledge.

The flexible nature of the simulation platform offered by Simulink allows simulation ease for modern optical communication systems. Maintaining a focus on developing the single channel DQPSK system by simulating the effects of real optical devices in our laboratory, such as transmitter configuration, Mach Zehnder modulators, optical fiber (propagation models) etc allow for direct translation to experimental configurations.

The simulator developed here is integrated with other Simulink models to facilitate the simulation of all aspects of a 10 Gb/s DWDM system by incorporating certain simulation components (i.e. EDFA, Fiber models) to compare with those obtained experimentally.

2. Optical Networks Classification

Since their first development and deployment, optical transmission networks o_er improved possibilities for dealing with ever growing demands on transmission bandwidth and system capacity. In the last 20 years, the optical transmission networks have become one of the most important part in the telecommunication hierarchy, whose seamless integration with conventional network applications and services forces a further development and a broader deployment of optical networks in all telecommunication areas. Making a classification of di_erent optical transmission networks, it can be distinguished between Access, Metro and Core (or back-bone) networks (Fig.1).[29]

This is the most convenient network classification made regarding to the transmission distance or network diameter. Access networks as the base of the telecommunication hierarchy, are characterized by the interaction between numerous di_erent network technologies based on di_erent transmission media e.g. wire, wireless or fiber [29].These networks possess a small total capacity and inter-operational functionality between di_erent transmission protocols (e.g. TCP/IP, ATM) and services (e.g. ISDN, DSL).

The conventional wire based data transmission dominates the access area, making these networks to become a bottleneck of data transmission in the future. The implementation and deployment of optical networks in this region e.g. fiber-to-the-home (FTTH) and fiber-to-the-business (FTTB) would address the bottleneck problems, hence enabling an even broader bandwidth access than with conventional wire based technologies (e.g. DSL). But this is rather a question of deployment strategy and cost than of the achievable transmission performance. Metro area networks (MANs) accumulate the tra_c from the access networks with di_erent protocols and services, enabling its further transmission over longer distances.[29]

The MANs are based on optical transmission technologies and they are characterized by a limited transmission distance (< 200 km) and an increased network complexity. Furthermore, MANs have to deal with di_erent communication protocols, thus requiring close interaction between the network management and transmission infrastructure, which results in the fact that the channel data rates used here are rather small (<10Gb/s/ch, at the moment).

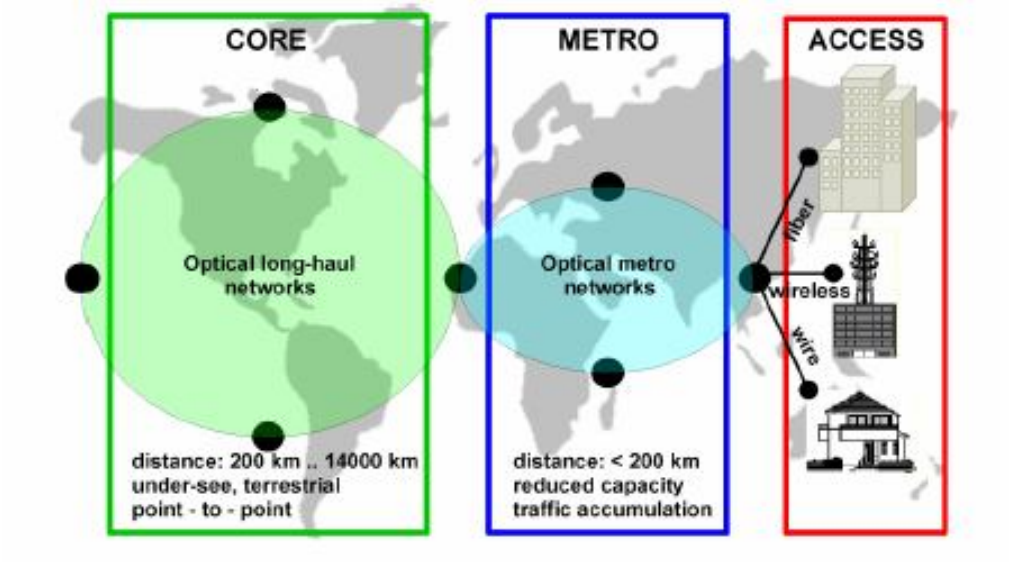

Figure1: optical Networks classification (1) [29]

3. 40 Gb/s WDM and DWDM investigations

3.1 General Idea

After investigation of 40Gb/s single channel transmission characteristics and highlighting dominant system limitations, the next step into the direction of future transmission systems is made considering multi-channel 40Gb/s systems employing the wavelength division multiplexing (WDM) technique. The numerical investigations taking into account various transmission aspects were performed in order to determine and describe the capacity upgrade mechanisms which could enable a better utilization of the available system bandwidth.

It is distinguished between WDM systems with a spectral efficiency smaller or equal than 0.4 bit/s/Hz, and dense WDM (DWDM) systems employing spectral efficiency larger than 0.4 bit/s/Hz. Since at the start of the works presented here, the realization of 40Gb/s DWDM systems was not sufficiently investigated by means of theoretical or experimental investigations, the design rules for spectrally efficient 40Gb/s DWDM systems are developed and presented in this work.

As representatives for WDM and DWDM systems, transmission systems with channel spacing of 100 and 50GHz have been investigated, corresponding to a spectral efficiency of 0.4 and 0.8 bit/s/Hz, respectively in the 40Gb/s case. The investigations presented in this chapter are made considering parameters of already available system components for intensity modulated direct detection systems. In order to concentrate on transmission effects and characterize system behavior, the investigated transmission lines do not contain any sophisticated technologies, e.g. super FEC codes or orthogonal polarization between adjacent channels.

The investigations were started with an optimization of filter settings of optical filters deployed in multiplexers and demultiplexers, which turn out to be an important issue for the DWDM system realization. After determination of optimum span lengths (amplifier spacing) for 4x40Gb/s based WDM/DWDM systems, power investigations were performed, which enable identification of optimum power settings in transmission and dispersion compensating fibers.

Using optimized parameters, the interaction between implemented
dispersion maps per span and transmission effects is analyzed, drawing conclusions for optimum dispersion compensation schemes both at 100 and 50GHz channel spacing.[29] The attained insights are used for the investigation of system total performance in WDM and DWDM cases over short distances (up to 4x80 km).

All works presented are conducted considering different ASK-based modulation formats, for enabling a fair comparison between them and identify advantages and drawbacks for each format. Contrary to the previous chapter, investigated modulation formats are divided into three groups: NRZ-based, RZ-based and novel modulation formats in order to stress their different linear and nonlinear propagation characteristics. [29]

The 40Gb/s multi-channel works are completed by long-haul investigations with transmission distances up to 10x80km, whose target was the determination of length dependent performance changes and accumulation of transmission disturbances in multi-span systems.

3.2 **Investigated system setups**

According to the aim of this work to investigate transmission performance of 40 GB/s based transmission lines and the system upgrade from single channel to WDM and DWDM transmission systems, the system infrastructure used for investigations presented in this chapter is similar to the setups used for single channel investigations. For both WDM and DWDM investigations, an identical transmission line infrastructure is used (Fig.1). The differences occur at the system edges i.e. the transmitter and receiver side, where multiple channels are multiplexed and demultiplexed. A typical system setup is depicted in Fig. 1.

The WDM channels are symmetrically arranged around a central wavelength of 1550 nm, and are modeled using different bit sequences with a length of 29 bits (see Appendix C). At the transmitter side, all channels are multiplexed by a MUX filter. The optimization of MUX filter bandwidths was performed in order to determine optimum filter settings for different channel spacing. The filtering losses of the MUX are compensated using an EDFA-based optical booster before the transmission line.

The investigated transmission line consists of identical spans employing transmission single-mode fibers and DCFs. The linear and nonlinear parameters in the transmission fibers were varied in order to identify optimum parameter combinations. As in the single channel case, the accumulated dispersion is fully compensated on a span-by-span basis. Besides pure post-compensation (Fig.1), further dispersion compensation schemes are considered.

The investigations are made over different transmission distances, e.g. 2, 4 and 10 spans. After transmission, WDM channels are demultiplexed and detected with a conventional 40 GB/s NRZ-based receiver. For the investigations presented in this chapter, 40 GB/s WDM/DWDM systems are considered. This number of channels enables an investigation of the most important inter-channel effects, e.g. XPM and FWM. The SRS effect is considered in the transmission line, but due to the reduced number of channels and the small system total bandwidth, it can be neglected.

The performance evaluation is done considering one of the middle channels as a worst-case channel, which is affected by strong multi-channel nonlinear limitations (e.g. XPM, FWM). Different evaluation criteria were used, e.g. Q-factor, EOP, and dynamic range, in order to give an insight into transmission limitations and enable a comparison between various evaluation criteria. For the investigations presented here, it was assumed that all channels are co-polarized.

3.3 Optimized optical filtering in WDM and DWDM systems

The right choice of the optical filter type used for multiplexing and demultiplexing in 40 Gb/s based WDM transmission systems is crucial, especially in systems with an increased spectral e_ciency [30], [31]. Narrow band filtering has to be employed both at the transmitter and receiver side for a reduced channel spacing (<100GHz). As stated in Chapter 2, narrow-band filters with sharp filter edges and flat pass-band characteristics represent the optimum solution for enabling DWDM transmission systems.

Such filters are already commercially available for channel spacing of 100 and 50 GHz. For the numerical investigations presented here, the characteristics of flat-top filters are emulated using Gaussian filters of higher filter order (2n) known as super Gaussian filters. The frequency response of super Gaussian filters is defined as:

$$T(f) = \exp(-\ln\sqrt{2(\frac{2(f - f_c)^{2n}}{f3dB})}) \quad (1)$$

where fc is the filter central frequency,
n defines the order of the filter,
F3dB represents the 3-dB optical bandwidth of the filter.

The filter responses of super Gaussian filter. It depicts the filter characteristics for different filter orders (n=2, 3, 4), showing that an increased filter order results in an increased steepness of filter edges. The realization of optical filters with steeper edges could represent a difficult issue, due to the more complex definition of filter parameters and filter phase delay characteristics [32], [21]

For the investigations presented here, 2nd order super Gaussian filters was used without consideration of their phase characteristics (e.g. filter dispersion, phase delay). These filters very well match the filter characteristics of conventional ”flat-top” array wave-guide grating (AWG) based filters, which can be practically used as MUX and DMUX. For numerical realization, MUX and DMUX consist of several super Gaussian filters.

After choosing a right filter type, it is necessary, especially for DWDM transmissions, to optimize the filter optical bandwidth (f3dB). The MUX and DMUX bandwidths per channel have to be adjusted and optimum bandwidth ranges have to be determined for the realization of DWDM systems with a spectral e_ciencyhigher than 0.4 bit/s/Hz. The filter bandwidth optimization is done considering back-to-back transmission and di_erent modulation formats for channel spacing (grids) of 100 and 50 GHz, respectively, because these values are already standardized representing the following steps in WDM system evolution.

In both cases, a symmetrical optical filtering is employed, meaning that the central filter frequency match the carrier frequency of the channel. It must be stated that the implementation of a MUX at the transmitter side for 100 GHz channel spacing is not essentially needed independent of the modulation format, because the channels can be multiplexed with conventional couplers without filtering capability, but in order to enable a better comparison between WDM and DWDM systems, and to highlight some system upgrade aspects, e.g. use of already deployed infrastructure, the WDM systems are considered with a MUX at the transmitter side.

Furthermore, it must be stated that the electrical filtering in receivers becomes important at reduced channel spacing [30], but due to the fact that implemented electrical filter bandwidth is quite large (28 GHz) it causes no additional penalty.

4. Optical Transmission Scheme over DWDM

Particularly for the enlarge in demand for transmission capacity of modern optical fiber communication systems, considerations into alternative methods which allow for this increase need to be evaluated.
There are existing two alternative options:

1. Improves transmission bandwidth by merely increasing the data rate. Current transmitters used in some modern optical fiber systems operate at 40Gbps. This approach can become moderately costly when used in systems with several data sources like video, data, etc.

2. Increases the number of transmitters (wavelengths) and thus the overall transmission rate by the same factor. Basically multiple wavelengths are transmitted on the one fiber. We consider for example, 20 channels operating at 10Gbps, each coupled in the one fiber making the overall transmission rate 200Gbps. With improving transmitter technology, DWDM systems employing 40Gbps narrow spectral spaced channels have also allowed T bps transmission to become a reality.

In this report we consider a single channel from the second alternative as the design of choice for the optical communication system, simulating a single channel from a DWDM system operating with 10Gbps per channel.

The foundations of the DWDM system rely on the ability to couple many wavelengths onto the one transmission link. Using commercially available optical technology such as optical de/multiplexers, optical amplifiers and transmitter diodes, a point-to-point DWDM transmission system can be developed as shown below in Figure 2.

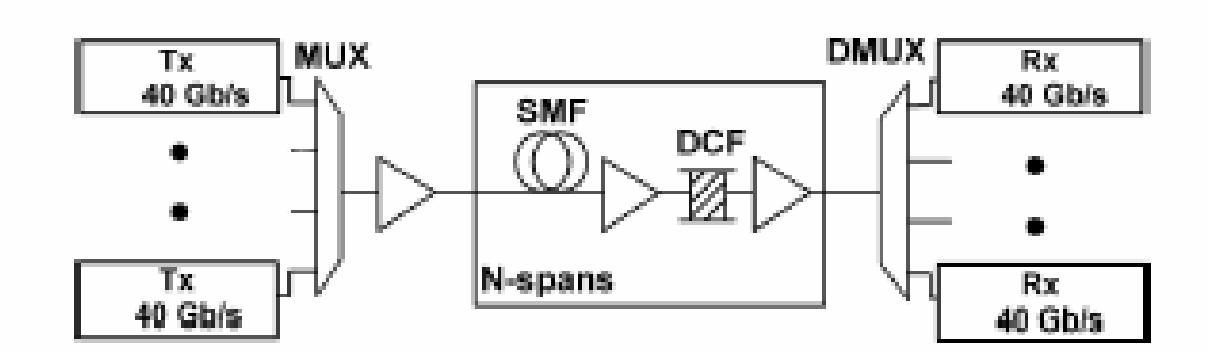

Figure 2: Architecture of DWDM transmission scheme

For the purpose of this report project we simulate only one Peer to Peer transmission channel link to understand the fundamentals of the DQPSK signaling technique. Our simulation model consists of various optical devices with there behavior represented initially by theoretical interpretation. For example, in the transmitter, the optical components are placed in cascade which effectively modulates the optical carrier signal using a DQPSK format. The details of the transmitter configuration will be outlined later. It is important to note here that the principle behind DWDM is to associate each transmitter to a different data stream or effectively a different wavelength.

Optical amplifiers, dispersion compensation modules and other optical devices may be added in between the fiber spans, this allows for long haul transmissions to be realized. These devices typically attempt to cancel any loss or attenuation in the signal as it propagates through the fiber.

The optical receivers (Rx) normally consisting of photo-detectors and other optical hardware such as a Mach-Zehnder Delay interferometer (MZDI) in the case of DQPSK transmission systems and other differential encoding systems. These optical devices allow for the demodulation of the received signal and allow measurements of bit error rate (BER) and other system performance parameters to be evaluated using the eye diagram monitored by the scope at an appropriate point of the system.

4.1 Overview of DQPSK Transmitter

Using the concept of feedback, the DFB laser is capable of providing a reliable single-mode optical carrier [7]. It is constructed using a cavity enclosed on by both ends by a

grating. Light is reflected internally in the cavity until the phase of an incident and reflected wave are matched. The light is then allowed to propagate. In this report we simulate the DFB laser diode using a signal generator.

Mach-Zehnder interferometric modulators (MZIM) are the most widely used as the photonic devices for external modulating the generated light-waves. Although several types of MZIMs exist, in this report project we consider the well known lithium niobate (LiNbO3) single electrode modulator based on its common use in 10Gbps PSK systems. Its role in most DWDM systems, and in this project, is to outwardly modulate the carrier phase via the electro-optic effects and is thus usually placed in cascade with a DFB laser. The MZIM consists of a Y splitter (3dB), two waveguide arms and a Y combiner as shown in Figure 3.

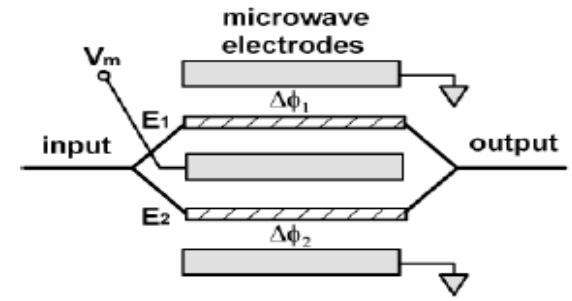

Figure 3: Mach Zehnder modulator

The electro-optic effect allows the refractive index of the material to change as a response to applied voltages E1 and E2. For single electrode MZIM also known as the modulating DataStream E1=0. The phase of the signal as it passes through this region of applied voltage binary or sinusoid ally is changed. At the input, the power of the incident carrier is split equally, one carrier wave experiences a phase change (0 or π red), while the other passes through unchanged, two waves emerge and interfere with each other at the output. It should be noted that the optical carrier that has experienced the 0 or π phase shift in the lower arm of MZIM, is of great importance since the differential phase of this waveform will represent the first encoded bit of the two bits (di-bit) to be transmitted.

The MZIM is also a useful device in its response to certain high bit rate pulse shapes NRZ, RZ, which can be used in replacement of a normal phase modulator (PM) biased to π phase shift. Other PMs simulated in this report operate under the same physical principles as the MZIM however are assumed to be biased to produce a π /2 phase shift in the optical carrier.

4.2 Overview of Optical Fibers line link

We just consider for our project the linear model for light-waves propagation in fiber[10]. Fibers allow digitized light signals to propagate without loss of signal for distances beyond 100 km spans with loss compensated by optical amplification [9]. Fiber technology has improved dramatically with attenuation levels reaching 0.25dB/km or better in the 1550 nm C-, L- and S bands [11].

Chromatic dispersion is a property of optical fibers which limits the performance of the optical fiber communication system. Chromatic dispersion is the effect of pulse spreading or broadening and can reduce the integrity of a received signal unless appropriate dispersion compensation modules or fibers (DCM / DCF) are included in the system design. Two types of chromatic dispersion exist:

Firstly, material dispersion is caused by the fact that multiple wavelengths different refractive indexes [12], the velocity of propagation in the fiber, given a wavelength dependent refractive index, is thus c/n(λ).

Secondly, effects of waveguide dispersion are heavily dependent on the geometrical characteristics of the fiber. Thus effectively there is a strong relationship between the relative refractive index and the normalized frequency parameter V[12]. Thus the bandwidth of an optically modulated signal influences the impairments due to propagation.

The polarization mode dispersion (PMD) is another important dispersion effect that introduces system power penalty. Although this parameter has only been observed experimentally [13], it can reduce the integrity of two adjacent pulses of transmitted data by introducing a third, unwanted pulse. PMD effects are integrated in another Simulink simulator.

The role of the chirp factor á, and in particular its influence on the performance of modern fiber optic systems is to be considered. Chirp, in particular transmitter chirp, is known to be a main contributor to spectral broadening [14], also limiting transmission to short distances (for α >0). Thus to minimize the effects of pipe, we have considered the sources of this effect.

4.3 Overview of DQPSK Receiver

The principle operation of this device is to convert phase-coded information, such as that generated by the DQPSK transmitter into an intensity signal which can be detected by a photodiode circuitry at the output of the delay interferometer (DI) arms. The intensity of the signal at the output of the DI arms is dependant on the phase difference between adjacent bits [15], $\Delta\phi_{\text{mod}}$ of the optical carrier in both the upper and lower arms, the relationship between phase and intensity is expressed as:

$$\mathrm{I}(\Delta\phi_{\text{mod}}) = 0.5\cos\left(\Delta\phi_{\text{mod}} \pm \frac{\pi}{4} + \delta\phi_{DI}\right) + 0.5 \quad] \tag{2}$$

Where $\Delta\phi_{DI}$ is a phase offset

Figure 4 shows the optical device structure. Note that this is a Mach-Zehnder device and thus operates on the principles of interference between the two arms which is dependent on the phase difference. For the applications of DQPSK demodulation, the delay T is one bit in length (100ps for 10Gbps operation) to allow for proper interference between two adjacent bits.

Effectively the delayed signal acts as a phase reference for the incoming symbol. The extra phase delay (phase = $\pm\frac{\pi}{4}$) is normally implemented in practice for DQPSK systems only using integrated thermal heaters.

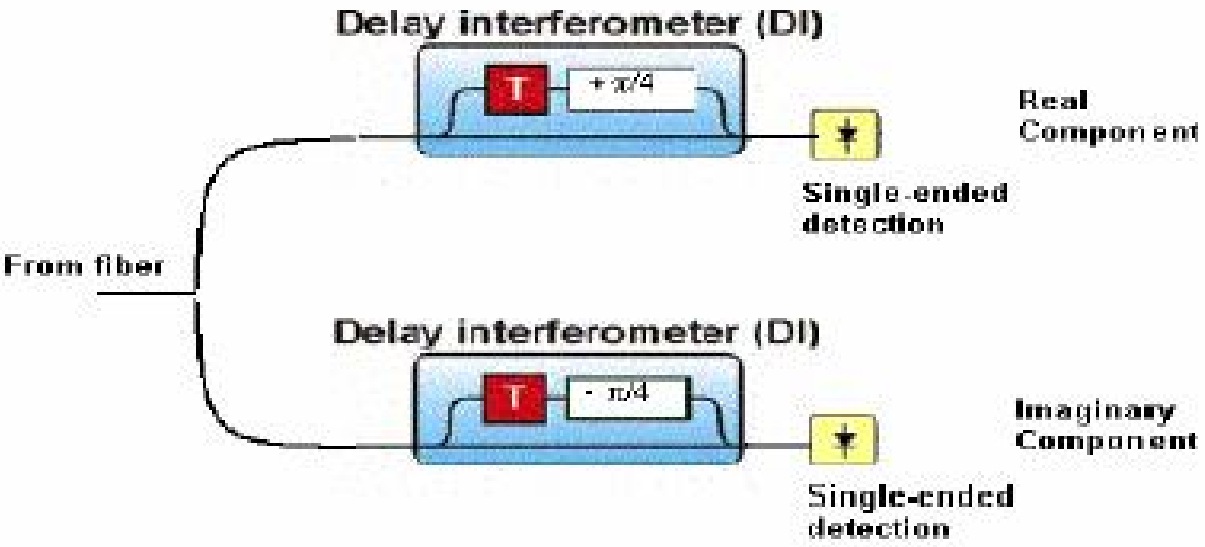

Figure 4: Delay interferometer[16]

5.Overview of DQPSK modulation format and Simulink simulator

When digitizing data for transmission across many hundreds of kilometers many digital modulation formats have been proposed and investigated. This report investigates the DQPSK (Differential Quadrature Phase Shift Keying) modulation format. This modulation scheme although having been in existence for quite some time had only been implemented in the electrical domain. Its application to optical systems proved difficult in the past as constant phase shifts of the optical carriers are to be maintained.

However, with the improvement of optical technology and alternative transmitter design setup, these difficulties are eliminated. One of the main attractive features of the DQPSK modulation format is that it offers both twice as much bandwidth and increased spectral efficiency compared to OOK. As an example, comparisons between 8 x 80Gbps DQPSK systems and 8 x 40Gbps OOK systems show that DQPSK modulation offers more superior performance (i.e. spectral efficiency)[5].

The very nature of the signaling process also allows non-coherent detection at a receiver to be possible, thus reducing the overall cost of the system design.

The DQPSK modulation format uses a differential form of phase shift modulation to the optical carrier which encodes the data. DQPSK is an extension to the simpler DPSK (Differential phase shift keying) format. Rather than having two possible symbol phase states (0 or π phase shift) between adjacent symbols, DQPSK is a four-symbol equivalent {0, π /2, π or 3 π /2}. Depending on the desired di-bit combination to be encoded, the difference in phase, $\Delta\phi_{\text{mod}}$., between the two adjacent symbols (optical carrier pulses) is varied systematically. Table 1 outlines this behavior.

Di-bit	**Phase difference (degrees)**
00	0
01	90
10	180
11	270

Table 1: DQPSK modulation phase shifts

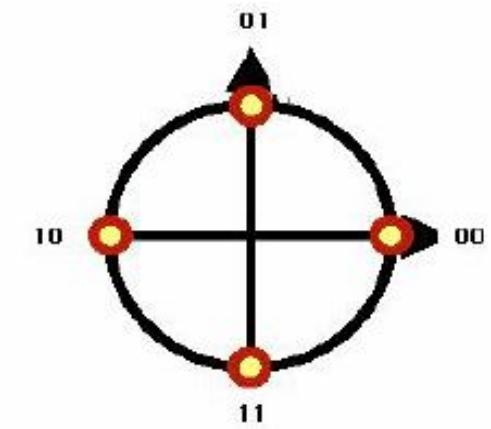

Figure 7: DQPSK signal constellation

Ideally the amplitude should remain constant and the phase of the signal is changed during transitions, however due to the characteristics of the optical equipment (i.e. MZIM) some form of optical intensity modulation should in practice also be observed. This is usually termed as the patterning effect. This effect is investigated, however not implemented in the final simulator due to data pulse representation inaccuracies.

5.1 Overview of SIMULINK Simulator

5.1.1 Sampling theorem for Digital pulse shape

Given this report has been implemented in the MATLAB subsidiary program SIMULINK, most of the data supported by the block sets can only support discrete data sources/ values. Thus a means of converting continuous waveforms to discrete values is required. Signaling theory states that a continuous signal s(t) can be represented by a set of samples taken at a sampling frequency f_s [20]. This sampling frequency must be at least twice that of the highest frequency contained in the signal waveform, B.

This is represented mathematically by:

$f_s \geq 2B$ Samples /second (3)

The value $f_s = 2B$ is referred to as the Nyquist rate. All samples made during the simulation are made at the Nyquist rate to ensure synchronization between data samples and to minimize sampling errors. As mentioned earlier the concept of pulse shapes in applications to the MZIM. We consider now the return-to-zero (RZ) digital signal, the pulse shape used in the final design of this report. This pulse shape has duration of half the period (T/2), thus has a 50% duty cycle. In most modern optical systems, this RZ pulse shape is often approximated by a sinusoid having frequency 1/T Hz [21].

The brief nature of the pulse, makes the RZ pulse shape more tolerable to inter symbol interference (ISI) compared to the non-return-to-zero (NRZ) pulse shape however its power spectra occupies a larger bandwidth. In this report we consider the RZ pulse shape as it is more compatible with the simulation development. The NRZ pulse shape also has a data rate of 1/T b/s however its duration is now T seconds. The power spectrum is also reduced to half that of the RZ pulse spectrum.

The final results displayed during simulations include the di-bit NRZ electrical bit stream (2 x10Gbps) which modulates the optical carrier via the MZIM and PM, the spectrum of the transmitted optical carrier, the RZ time-domain pulse generated and finally the eye diagrams both before to fiber propagation and after to allow for BER testing and other system performance measurements. We now consider each block shown in Figure 8 and present the development process.

5.1.2 Formation of the simulator models

With adequate knowledge and theory of the optical components required in the design of a single channel 10Gb/s DQPSK transmission link we can now consider the development process of the optical simulator. This simulator considers only one channel implementing the differential quadrate phase shift keying (DQPSK) signaling technique (total 20 Gb/s data rate); multiple channel configurations (DWDM) have been considered as future work. The primary design of a single channel operating efficiently was considered critical.

We have developed this simulator package in three main steps, each relating to the three main components in the transmission link. These include the transmitter, fiber and receiver models.

As this report focuses on the optical signaling technique DQPSK ever attempted in Matlab Simulink, especially how this signaling technique can be implemented in the optical domain using photonic hardware is essential. The work done uses a previously developed Simulink simulator [22] for implementing the OOK format as a guide.

The transmitter performing the DQPSK transmission format is developed first. This digital signaling technique can be implemented several ways using different hardwires. The final technique chosen proved to be the simplest to design and simulate using conventional data processing blocks in Simulink. The configuration of this transmission system is also partially based on the published works on DQPSK signaling transmission [5]. Figure 8 shows the top level of the single channel optical DQPSK Simulink model developed. This model can be later altered and new blocks added to optimize the system to individual requirements.

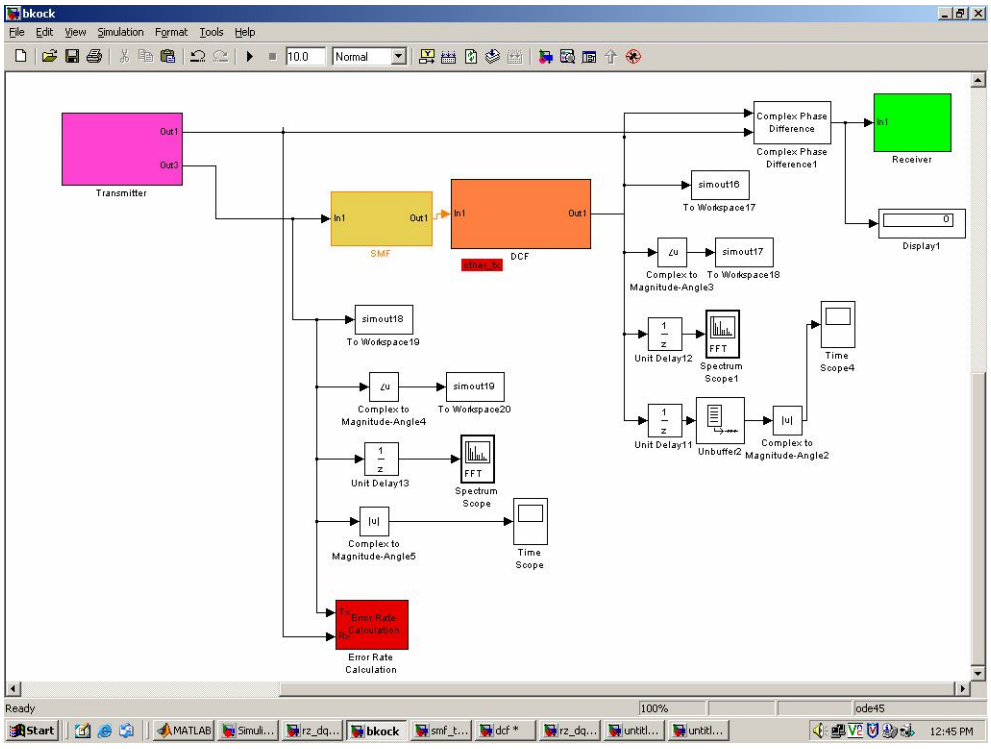

Fig-8: RZ-DQPSK transmission Simulink optical Simulator for single channel.

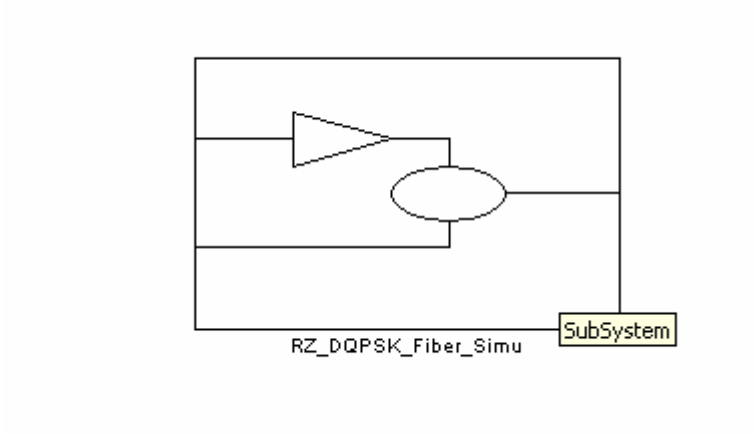

Fig 8.1: Subsystem of our Simulator for single channel.

5.2 Parameters using for the Simulator

Parameters	length	dispersion
DSF	80000	3e-6
DCF	16000	-85e-6
SMF	80000	
Carrier Frequency	1.94e14 Hz	
Wave length	1550nm	
Bit rate	10 GHz	
Bit num	256	
Speed of light	3e8 m	
Sampling (t)	2.59e-15 s	

Table: 2 Parameters list

5.2.2 Block series Transmitter model

The transmitter is an integral component in any optical fiber communications system and thus we have given the transmitter design first priority in our simulations. Given that we have understood the operations of several key optical devices, we can specify the DQPSK transmitter model. The transmitter design is based on a design previously tested experimentally [5].

First we implement a RZ pulse carving MZIM which generates the RZ pulse shape desired. Next a generating 0 or π phase shift of OC is to be coupled along with a Phase modulator (PM) which induces a 0 or $\frac{\pi}{2}$ phase shift of the optical carrier.

When placed in this configuration the four phase states of the OC required by the DQPSK modulation format, {0, p/2, p or 3p/2}, can be achieved. Both the MZIM and PM are to be driven by random binary generators operating at 10 GB/s. Figure 9 shows the schematic diagram of the system transmitters for the RZ-DQPSK modulation. We originally started with the NRZ-DQPSK design however the RZ format is used more readily in practice and has proven to be more robust to system non-linearities30. **Figure 10** shows the Simulink model of the transmitter.

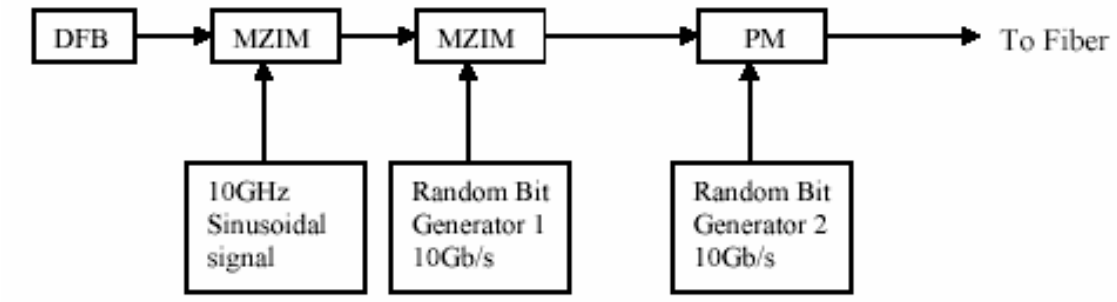

Figure 9: Schematic of a channel implementing RZ-DQPSK modulation**.**

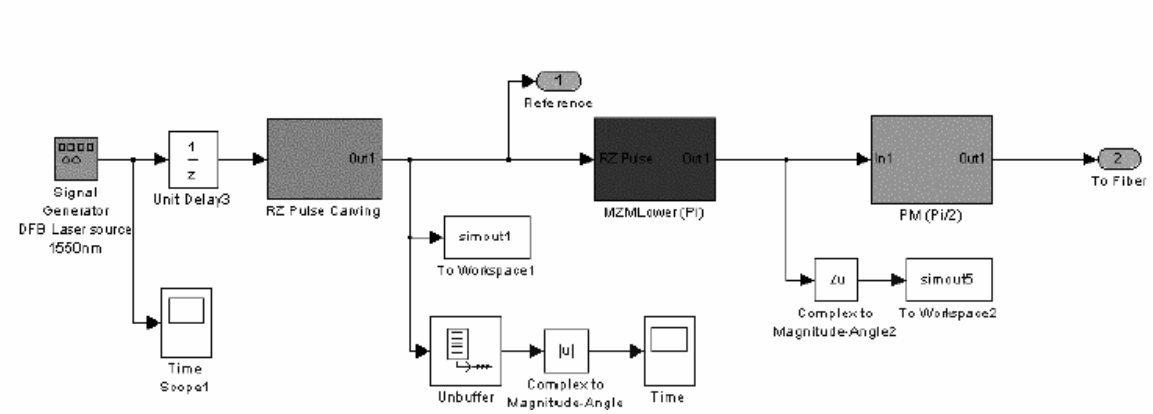

Fig: *Figure 10: Simulink mode RZ-DQPSK Transmitter.*

5.2.3 Optical carrier source model

As mentioned earlier, to simplify this part of the simulation development we are considering an ideal laser source (i.e. no frequency chirp present) and implement this in Simulink by selecting the "Signal Generator" block, represented by the block shown in Figure 11.

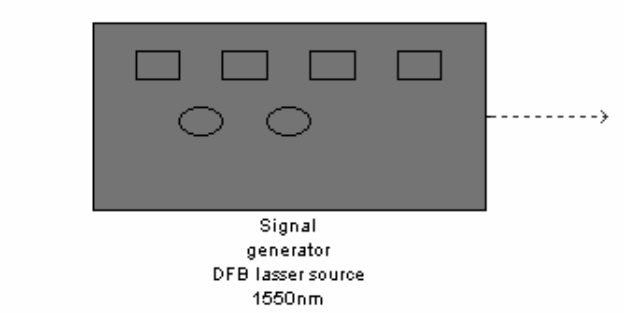

Figure 11: Signal Generator block in Simulink

This block models the desired sinusoidal optical carrier obtained from an ideal DFB laser which takes the mathematical form:

$$c(t) = A\cos(\omega_n + \phi) \qquad (4)$$

Where ω_n and φ are the frequency and phase of the optical carrier respectively, with

$\omega_n = 2\pi$ x 1.93×10^{14} red/.s

corresponding to the 1550 nm operating wavelength. A is the amplitude of the optical carrier has been normalized for simplicity and is thus set to unity. According to the Nyquist theorem, this sampling interval is at least twice the highest frequency in the system. Thus:

$$f_{sampling} \geq 2B$$

$$\mathrm{T}_{sampling} \leq \frac{1}{2B} s = 2.59 \times 10^{-15} s \qquad (5)$$

RZ pulse carving

The DQPSK transmitter performs a RZ pulse carving operation of the optical carrier lightwaves.This technique uses a sinusoidal driving voltage (10 GHz signal used as approximation to RZ pulse shape for 10Gbps system to drive the MZIM. This driving signal, a 10 GHz sinusoid is modeled here by

$$u_{2RZ-MZIM}(t) = \frac{1}{2} + \frac{1}{2}\sin \omega t. \qquad (6)$$

When multiplied by π gives a value between 0 and π. This value is used to implement the required phase shifting of the optical carrier (in the lower arm) resulting in a pulse waveform that oscillates between maxima and minima with 58% duty cycle as shown in **Figure 12**.

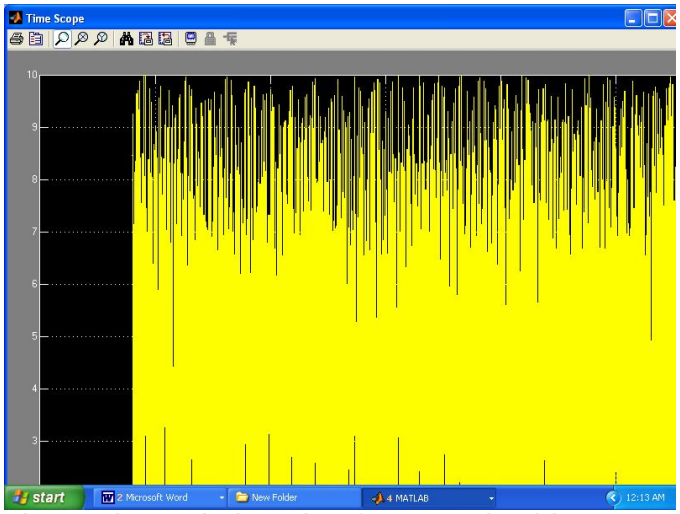

Fig 12: The Optical Carrier after RZ Pulse driven By 10 GHz

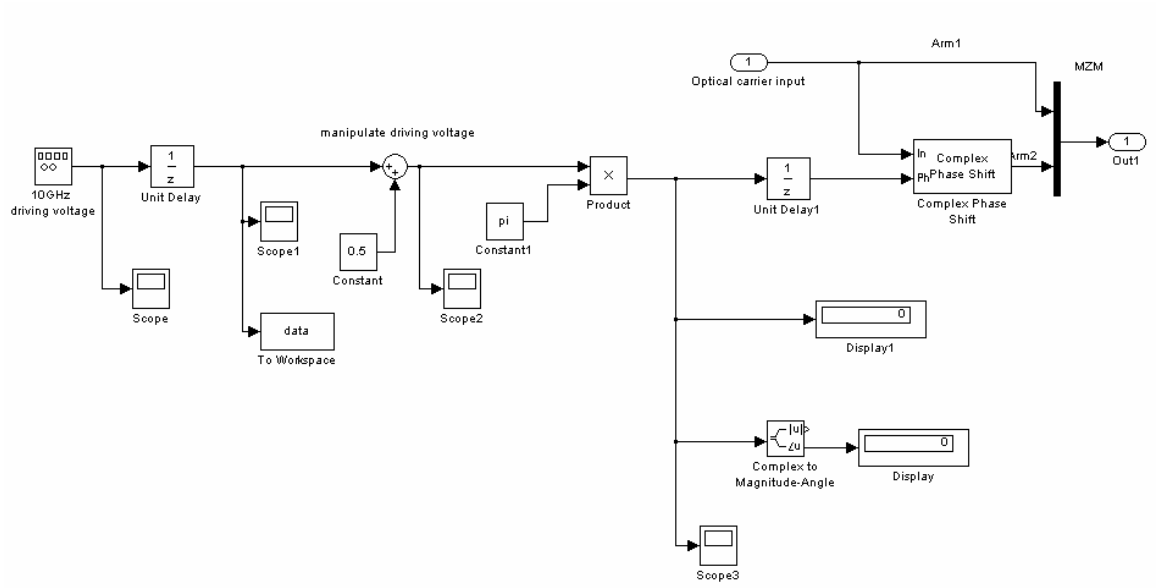

Fig:14 The simulink RZ MZIM Model

The MZIM driving signal given by (8) is constructed using a 10 GHz signal of magnitude 0.5; we add 0.5 and multiply these values by π. The values injected to the 'Complex Phase Shift' block 'Ph' input has value between 0 and pi as described earlier. This block then phase shifts the optical carrier at the 'In' port by the amount of 'Ph'. This signal is then added to an unaltered optical carrier simulating the Y recombine of the MZIM. The signal shown in Figure 14 is then passed to the second MZIM and the PM for phase modulation.

Overview of MZIM and PM models

In DQPSK transmission the second MZIM is commonly used as a 0 or p phase shifting device when biased at the minimum transmission point. Ideally a PM modulator, biased to produce a ð phase shift would be used however these are expensive and do not operate well at high bit rates in practice. Thus as a substitute the MZIM, which is very responsive to 10 or even 40Gbps systems is used in practice and thus used in our simulations.

The splitting of the optical carrier at the input of the MZIM thus causes the output, when viewed experimentally, to consist of two optical waveforms beating together, provided there has been some phase change in the lower arm. Thus in reality, it is the optical signal from the lower arm that is of greater importance as it has been phase shifted by E_2 (refer Figure 2). Although the sinusoidal carrier has been reduced by 3 dB due to splitter, we assume for simplicity that it retains its initial input power.

Thus in this report we only model the signal propagation through the lower arm of the MZIM, that is, the carrier will only experience either a 0 or ð phase shift depending on the value of the digital driving voltage signal (‘0’ or ‘1’ from Bernoulli block, refer to Figure 15).

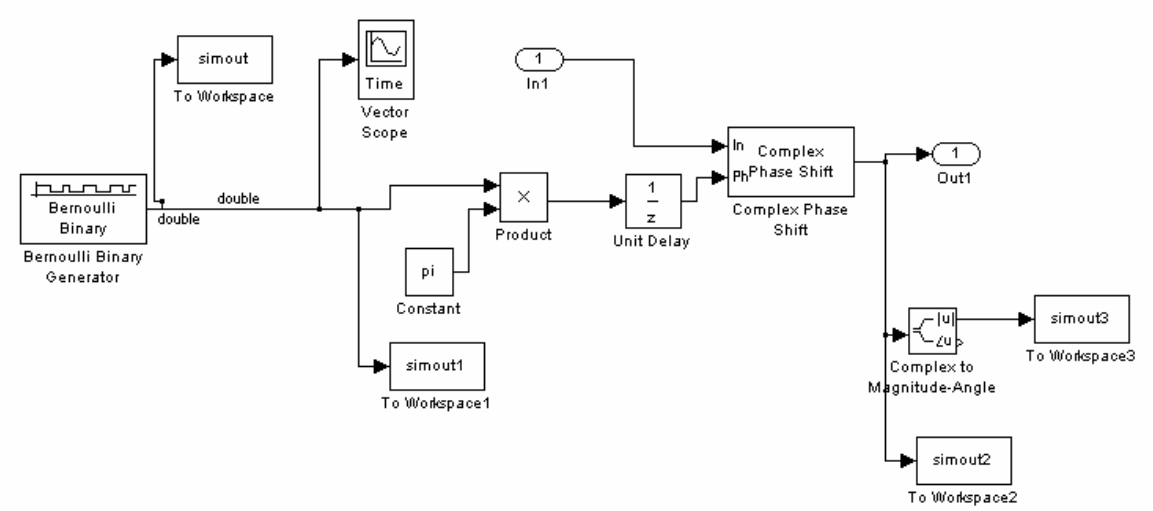

Fig:15 MZM Lower arm with pi phase shift.

The ‘Bernoulli Binary’ block generates a NRZ random bit pattern which when multiplied by π generates a value of either $\{0, \pi\}$. This value is sampled every bit period (via unit delay block every 100ps for 10Gbps operation) and the RZ-pulse carved optical carrier is phase shifted by 0 or π accordingly.

The Phase Modulator (PM) of the optical simulator operates on the same principles as the MZIM model, multiplying the random NRZ bit-stream by $\pi/2$ instead of π. We also consider a different bit stream to that driving the MZIM.

As can be seen in Figure 16, there is an extra ‘unit delay block’ at the output of the Bernoulli Binary generator, effectively delaying the original bit stream by one bit period. This ensures that the data driving the PM is ‘uncorrelated’ from the data driving the MZIM and that all four phase states of the signal constellation is achieved at some stage during simulation run-time.

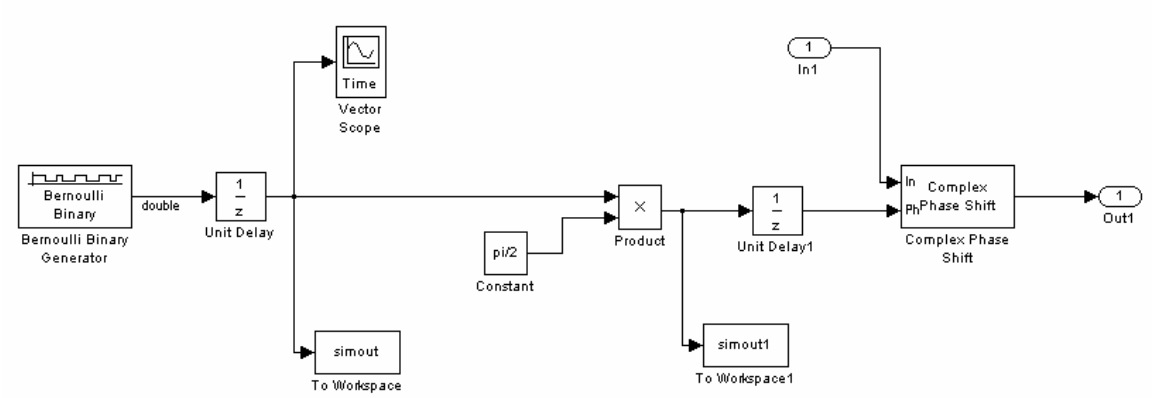

Fig: 16 PM Simulator Model.

In practice the characteristic of uncorrelated data is achieved by the physical time delay due to signal propagation between the second MZIM and the PM or using complementary data streams [5]. As shown in **Figure 10**, when the RZ pulse carver MZIM, an MZIM and PM driven by NRZ electrical signals are placed in cascade they modulate the optical carrier according to the DQPSK modulation format as required.

5.2.4 Overview of Linear fiber propagation model

Since the single channel RZ-DQPSK transmitter has been modeled, one can focus on the Simulations of the signal propagation via the optical fiber. There have been several fiber models which have been proposed. An example of these proposals includes the 'Fiber split step model' [23] which models the linear and non-linear phenomena in the fiber as the two optical temporal lenses and a nonlinear operator in the frequency domain.

Our developed model achieves this propagation accuracy by implementing fiber dispersion effects using time-domain digital signal processing and filtering technique that has been proven to be efficient in it computational resources. The split step model has been implemented in a report [22] and thus we consider an alternative fiber propagation model which considers the effects of dispersion on the system performance.

Dispersion management in high capacity (>10Gb/s) optical networks is of great importance, thus we consider predominantly the effects of dispersion in this model and later analyze the effects of different dispersion management techniques by inserting dispersion compensation fibers of varying dispersion factors (ps/nm.km). We also consider the effects of fiber attenuation with values based on standard attenuation levels of modern day single mode optical fibers (Corning SMF-28).

This fiber model assumes that the SMF can be represented as a band pass filter. The flat amplitude response in the pass band was initially presented in the literature however as an extension we have considered the effects of attenuation to simulate true fiber propagation. The final mathematical representation of the fiber is derived by first considering the slope of the group delay whose dependence on the chromatic dispersion is given by[24]:

$$\frac{d\tau}{dv} = \frac{d\tau}{d\lambda}\frac{d\lambda}{dv} = \left(\frac{-1}{L}\frac{d\tau}{d\lambda}\right)\left(\frac{\lambda^2}{c}\right)L \quad \text{Where} \quad \frac{-1}{L}\frac{d\tau}{d\lambda} = D(\lambda) \tag{7}$$

Here,

L is the fiber length,
λ the operating wavelength,
V the optical frequency
C the speed of light.

From these equations it can be shown that the equivalent model for the single mode fiber is expressed by the transfer function:

$$H(f) = e^{-j\pi D(\lambda)\frac{\lambda^2}{c}Lf^2} = e^{j\pi D(\lambda)Lc} = e^{-j\pi D(\lambda)\lambda Lf} \quad (8)$$

Since (8) is in the form of a frequency domain transfer function, it is more convenient to operate in the frequency domain as apposed to taking the convolution in the time domain. Determining the output of the fiber $X^{\wedge}_{out}(f)$ out given an input modulated signal $X^{\wedge}_{in}(f)$ in X f (where the ^ symbol refers to the Fast Fourier Transform (FFT) of x_{in} and x_{out}) is found by:

(8) is represented in block diagram as below in Figure 17.

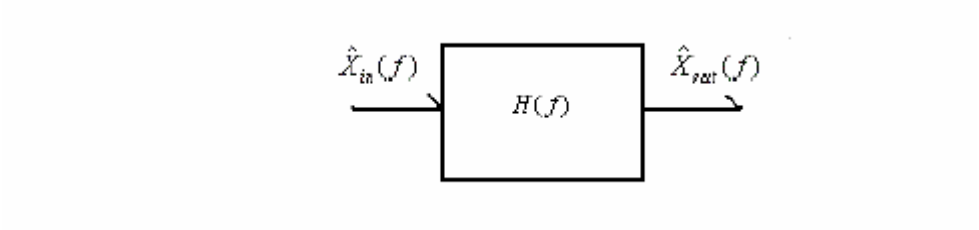

Figure 17: linear fiber model, low pass filter.

Thus by taking the FFT of the input modulated signal in Simulink then multiplying by H(f) and finally taking the IFFT (inverse FFT) we can accurately represent fiber propagation with any additional chromatic dispersion, thus making the model linear. For the standard SMF fiber model we use $D(\lambda)_{SMF} = +17\, ps/nm.km$ at 1550 nm wavelength, L = 80km with no optical amplifiers and for the dispersion compensation fiber (DCF) model we assume smaller length where, $D(\lambda)_{DCF} = -85$ ps/nm.km, L = 16 km. This value of dispersion for the DCF cancels the dispersion effects of the SSMF and ensures that there is no or little loss of signal phase integrity at the receiver end.

Given the Corning fiber SMF-28 manufacturers specifications quote an attenuation level of 0.2 dB/km; this implies a total of 16dB attenuation of optical power after 80km. This results in a power attenuation (Simulink gain block) of 0.03. This value is taken into account in the simulations as shown in Figure 18 of the SMF Simulink model via the Gain block at the top of the model.

Other fiber models are identically the same with modifications to the parameter values made as desired for dispersion compensation. It is possible to change the fiber parameters in the model directly though it is suggested that the parameters be changed in the initialization file mentioned in 5.1 and the simulations run again with the new changes.

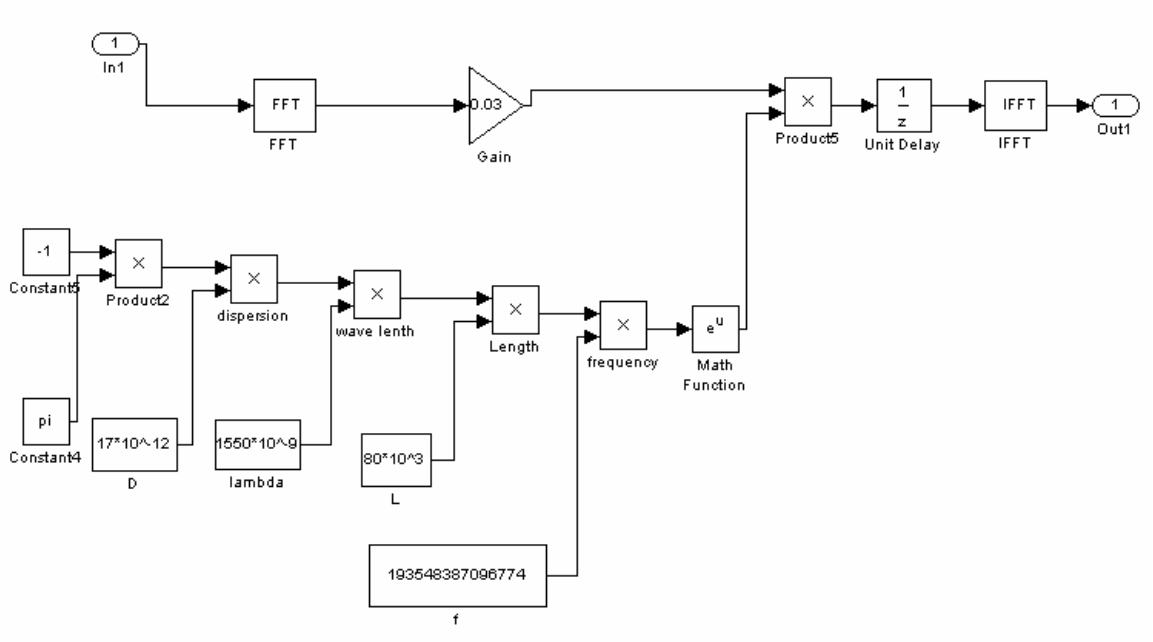

Fig:18 SSMF simulink model (FFT and IFFT)

It should be noted that no fiber non-linearity have been included in this fiber model.
Due to time limits the fiber model is considered to be enough for the needs of propagation modeling along with the effects of dispersion. It is suggested that the non-linear effects be considered for future work where effects such as self phase modulation (SPM) need to be considered. In this context we would need to consider the non-linear parameter γ , where γ is given by [25]:

$$\gamma = \frac{25\pi n_2}{\lambda A_{eff}} \qquad (10)$$

Where A_{eff} is the core effective area of the fiber and is given by $2\pi r_0^2$ where r_0 is the fiber spot size? The parameter n_2 is known as the material non-linear refractive index and takes the value $2\times10^{-20} m^2/W$. This nonlinear factor is thus known to produce a nonlinear phase shift which is dependant on the input power Pin by [6]:

$$\phi_{NL} = \gamma P_{in} L_{eff} \qquad (11)$$

Where Leff is the effective length of the fiber. To remain in a linear region of fiber propagation and minimizing the effects of SPM it is recommended that $\phi_{NL} << 1$ [6]. In addition to the fiber model developed in Figure 18 an additional non-linear phase ϕ_{NL} can be added in the case where $\phi_{NL} > 0.1$ say. A test of the value of ϕ_{NL} , which is dependant on the input power Pin as shown in (13) can be performed and added into the model based on the results of the test. With this addition, the effects of SPM on system performance could be assessed.

5.2.5 Over view of Receiver model

Based on the physical setup used in practice, this model of the DQPSK receiver attempts to simulate, to within Simulink capabilities, some of the key principles allowing for the successful decoding of the DQPSK modulated signal. We also place an exact receiver model (block: Post TX tap) before fiber propagation to allow for comparisons between pre and post fiber effects in eye diagram form. The scheme below is found to be regularly used for the modulation scheme mentioned previously in the transmitter component of this report.

Note that due to the differential nature of the modulation process, the demodulation and detection stage can be considered as a 'non coherent' or 'Direct Detection' scheme. The absence of a local oscillator (LO) and any other extra photonic hardware (i.e. mixers etc) required in conventional detectors makes this demodulation technique attractive. Indeed this detection process is the self-homodyne detection scheme.

The receiver configuration used in this report is capable of demodulating the signal transmitted along the 96 km dispersion compensated fiber span. Since the modulation format used in this report typically encodes two bits of data per symbol it is necessary to extract both bits (termed 'real' and 'imaginary' bits [5]) from the one received symbol.

We now outline the purpose of the $\pm \pi/4$ additional phase shift of the optical carrier implemented in the MZDI found in the receiver. Since the two bits to be encoded at the TX are implemented via an MZIM (0 or π phase shift) and the second bit is encoded via the PM (0 or $\pi/2$ phase shift) the two devices are said to be in 'quadrature' to one another. This implies that there is a $\pi/2$ phase difference between all signaling phase states, refer Figure 7. The additional + $\pi/4$ and - $\pi/4$ give a total $\pi/2$ phase difference between the upper and lower receiver branches shown in **Figure 20**.

Thus if data recovery was a main issue we could compare the real and imaginary bits received to those transmitted. However in this report we only consider the 'real component' received signal and asses the overall performance of the system via eye diagram analysis (using Q-factor method and BER).

In practice demodulation of the DQPSK signal uses the two branch configuration in Figure 19 has been successful [18]. A balanced detection set up has proven to be more sensitive and 3 dB improvement as compared with one photodiode detection scheme. We present here the detection using a single photo-detector. Balanced receiving system will be simulated in future work and the performance of sensitivity and BER is compared to the results obtained in this report. Thus the receiver model developed in Simulink is as shown below in **Figure 20**.

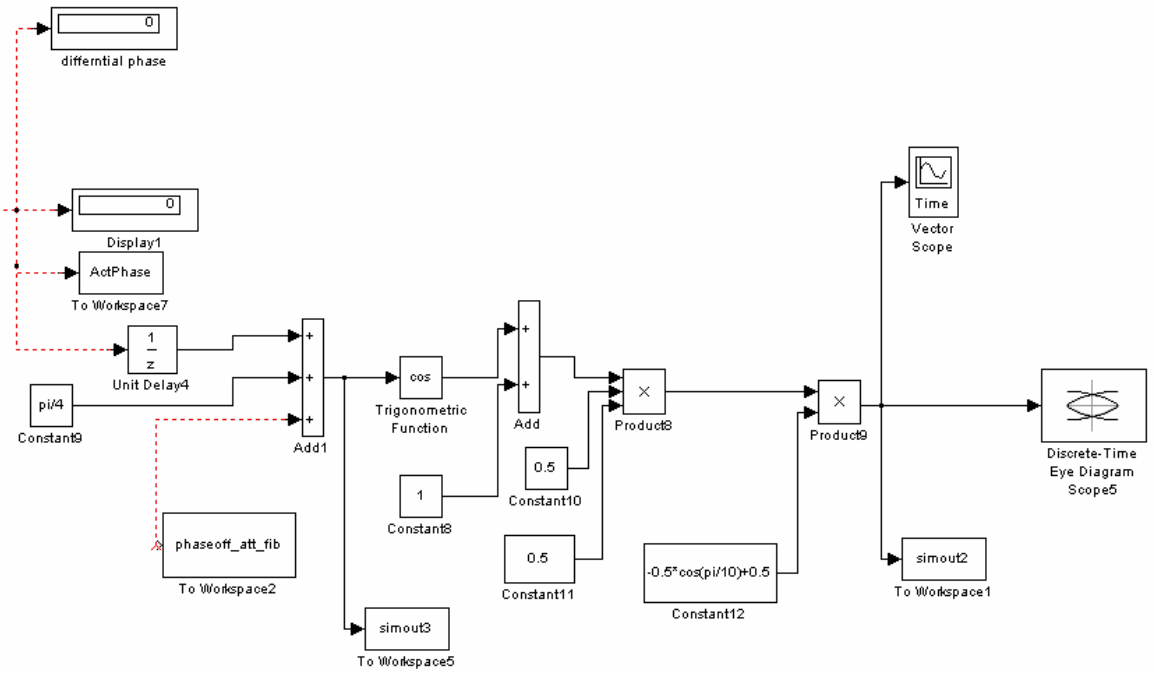

Fig: 20 DQPSK receivers Model

Mach-Zehnder Delay Interferometer model component

In Figure 8 it can be seen that at the input of Receiver block, there is a 'Complex Phase Difference' block. The purpose of this block is to deduce the overall phase difference between the received symbol that has been phase encoded and the reference signal given by the state of the optical carrier prior to modulation directed from the transmitter. The output of this block is constantly varying due to the periodic nature of the optical carrier; however we eliminate this problem by sampling this 'Phase difference' value every 100 ps for 10Gbps operation. This sampling is done by the first unit delay block observed above in **Figure 20**.

The reasoning behind this operation is to extract the optical phase difference (differential phase information) between adjacent symbols and to thus perform the phase to intensity conversion operation of the MZDI. This characteristic of the MZDI allows for the phase coded information to be converted into detectable intensity information [15].

Since we are only considering the real component of the received signal we need to add and extra + $\pi/4$ phase shift to the phase difference, $\Delta\phi_{\text{mod}}$ of the signal received. As shown in figure 7, when considering the four possible phase states of the DQPSK signaling format $\{0, \pi/2, \pi, 3\pi/2\}$ and adding DI phase of $\pi/4$, the overall phase difference takes 'equivalent' values of either $\{\pi/4$ or $3\pi/4\}$.

Given the MZDI transfer characteristic this leads two possible 'Intensity mappings' as Shown in Figure 21. From the values of phase obtained here we determine the corresponding output intensity of the MZDI by its characteristic expressed as:

$$I = 0.5\cos(\Delta\phi_{\text{mod}} + \Delta\phi_{DI} + \delta\phi_{DI}) + 0.5$$

Where $\Delta\phi_{DI} = +\frac{\pi}{4}$

The final term, $\delta\phi_{DI}$ in (12) is referred to as the phase offset. This additional phase originates from the MZDI and adds extra phase noise to the system. This effect is shown to reduce eye opening and hence degrades system performance.

We have interpreted this effect as being a result of the instability of the heaters which induce the required + $\pi/4$ phase shift, thus producing random values about this bias value. We have modeled this effect in Simulink by assuming a maximum possible value of $\delta\phi_{DI}$ and use a random 'Gaussian White noise generator' with small variance to represent this phase offset noise.

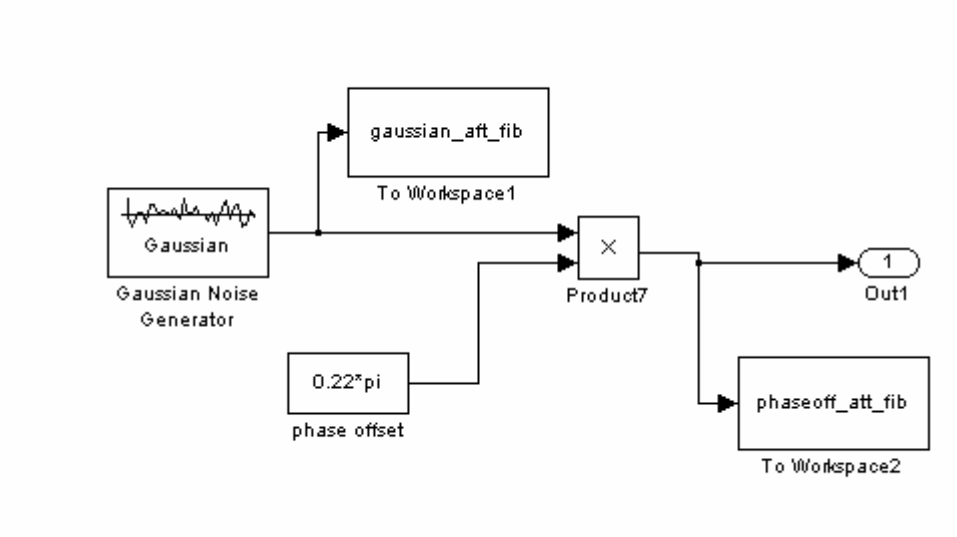

Fig:22 MZDI phase offset noise model.

The Photodiode Model component

Now that we have the intensity equivalent of the phase difference, we need to represent the optical to electrical conversion performed by the single-ended photodiode. From (2) we need to multiply the power, effectively the value just obtained from the MZDI, by the photodiode Responsively, We use a value of 0.5A/W obtained from Discovery Semiconductor Inc DSC10H PIN photodiode datasheet.

Evaluating the average photocurrent given a signal of power P from the MZDI using (2), we obtain one value between 0 and 1 as normalized current is assumed. Since we would like to asses the eye diagram generated by the received 'real' bits, we approximate the eye diagram pattern by the I pulse variable in our simulations.

Since the MZDI characteristic is cos-like, we assume the current waveforms forming the eye-diagram are cos-like also. The I pulse variable is expressed as:

$$I_{pulse} = -0.5\cos(t) + 0.5 \quad ; \quad 0 \le t \le 2\pi \tag{13}$$

We thus multiply the value of current obtained by (12) as shown in **Figure 23**. As each symbol is received and demodulated a waveform of type I pulse with peak value given by (2) will appear in the Time Vector Scope.

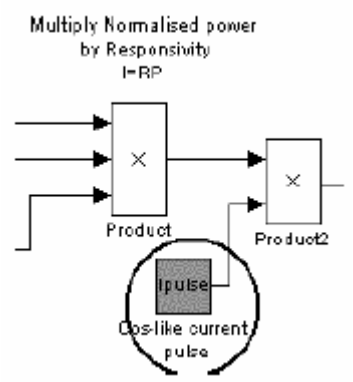

Figure 23:I pulse simulator for waveforms.

Photodiode/ Amplifier Noise component

The detection of transmitted light waves is performed primarily by the photo detector. In most instances, the received optical signal is quite weak and thus electronic amplification circuitry is used, following the photodiode, to ensure that an optimized power signal-to-noise ratio (SNR) is achieved [26]. This power signal to noise ratio is calculated as follows:

$$\frac{S}{N} = \frac{I_{sig}^{\ 2}}{\langle I_{noise}^{\ 2} \rangle} \tag{14}$$

Here we denote I_{sig} as the photocurrent and $\langle I_{noise}^{\ 2} \rangle$ as the mean squared noise contributions from the photo detector, the reason why we consider the mean squared noise will be explained later. Since one of the primary objectives is to best model optical components used in real experimental conditions the effects of noise is modeled. In particular the PIN photodiode and receiver total noise are calculated and superimposed over the ideal photodiode signal current.

Three sources of noises include: the quantum shot noise i_{sh} , the PD dark current noise i_{dk} and the thermal (Johnson) noise i_{th}. The total current generated by the photodiode when optical power falls on it is expressed by:

$$i_{total} = i_{sig} + \sqrt{\langle i_{noise}^{\ 2} \rangle} \tag{15}$$

Where $\langle i_{noise}^{\ 2} \rangle = \langle i_{sh}^{\ 2} \rangle + \langle i_{th}^{\ 2} \rangle + \langle i_{dk}^{\ 2} \rangle$

The noi8se source is expressed as:

$$\langle i_{sig}{}^2 \rangle = 2qI_{sig}B$$

(16)

$$\langle i_{dk}{}^2 \rangle = 2qI_{dk}B$$

$$\langle i_{th}{}^2 \rangle = \frac{2kTB}{R}$$

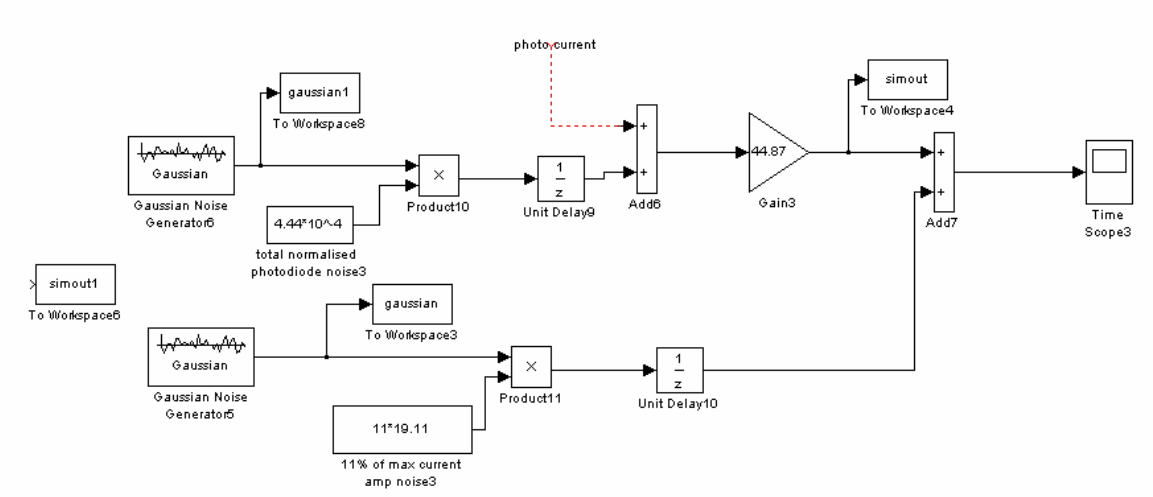

Fig 24: Photodiode / Amplifier noise Model

6. Single Channel DQPSK system simulator

In this section of the document we state the necessary steps required to operate the single channel DQPSK optical fiber communication simulator. Our intentions are to provide all the necessary instructions on how to alter the simulator for optimum individual requirements. The flexible nature of Simulink, and thus this simulator allows the system to be customized to handle different fiber types, and can with simple alteration of the transmitter and receiver even implement the DPSK modulation format.

This simulator was designed for DQPSK transmission in mind and is thus unable to support other modulation formats. However certain components from this simulator may be used to generate new simulators implementing alternative modulation formats.
This section present some results performed for assessing the overall system performance.

It includes an analysis of the effects of chromatic dispersion induced by the fiber model. We investigate the effects of dispersion compensation fibers in the transmission link, in particular the effect of phase distortion by comparing the received phase difference to the expected phase difference originally encoded in the symbol. We also perform BER testing derived from the eye diagram generated by the Q-factor.

6.1 Operating the DQPSK OFC Simulator

The simulator operation has been designed based on a previous Simulink simulator design [22]. This report uses the principles of operational simplicity to allow for ease of operation and flexibility for the user. It is important that prior to running any simulations the initialization file contained within the simulation package be run.

To begin running any simulations open Matlab™ 7 and open the file initialize optical simulator DQPSK .m Some of the variables made available to the user for alteration include transmission bit-rate, dispersion factors and length of various fibers. By localizing all the variables used in the simulator in the m-file allows the user to make system or fiber alterations to the m-file and consequently result in an update of variable in the simulator once the simulator is re-initialized.

All the variables declared in the initialization file will automatically be placed on the Matlab workspace. If these variables are not declared and defined prior to simulation run-time Simulink will generate errors. After running the initialization file, the DQPSK simulator model is automatically open, provided the user has specified the correct file location of the simulator file named RZ_DQPSK_simulink_opt_fiber.m, in the open command at the end of the m-file.

Now that the simulator has been initialized with all the fiber parameters and bit-rates etc, simulations can now begin. To begin simulations click the - button on the Simulink toolbar, or click Simulation. Start. All the vector scopes, spectrum scopes and eye diagram windows are open. These windows present a graphical representation of the processing of data in real-time. Users can observe certain phenomena whilst also acting as a good guiding tool to troubleshoot any underlying system problems.

During the simulations, data generated by the simulator is stored in the Matlab workspace variables. At the conclusion of the simulations this data can be analyzed and processed in Matlab to present other graphical representations of the results as desired. To observe or alter the contents of each sub-block in the simulator model simply double click on the block of interest and the contents are revealed.

6.2 Performance DQPSK optical simulator

The SOAST has been designed to be as flexible as possible to allow users modifications of system parameters, and to add or remove simulation blocks as desired. For example one may need to alter the current state of the simple transmission peer to peer transmission link by forming long-haul transmission with optical amplifiers and improved dispersion management.

The applications of this simulator are left to be user specified. However for testing purposes and to give an indication of the proper operation of the 10Gbps single channel DQPSK system, we consider two system configurations.

One utilizes standard TX and Rx whilst assuming SMF type with no dispersion management, the other includes dispersion management in the form of a dispersion compensating fiber (DCF) module. Thus the overall transmission span is 96 km. This fiber span corresponds well with the typical transmission distance considered in practice (<100 km).

The system parameters used in the following simulation correspond to the values specified in the initialize optical simulator DQPSK m file shown in the Appendix 8.1. After running this initialization file and loading all variables into the Matlab workspace the simulations can now begin (after clicking the run, button), the following window scopes (refer Figure 26) open to display appropriate data signals. The simulator displays the following window scopes in real time:

- MZIM and PM NRZ electrical random data driving signal;
- Optical power spectrum of single channel (193.4 THz = 0.1934 PHz; PHz = 1015 Hz) post transmitter and at receiver inputs;
- Single photodiode electrical current eye diagram scope at the receiver with no Photo diode/amp noise; and
- Single photodiode electrical current eye diagram scope post transmitter, and at the receiver
- Super imposed by all noise sources.

Other time scopes in the simulator system can be manually opened during simulation run-time. A large number of windows have been assigned to open automatically. The importance of certain data representation is left to users and can be disabled if required. However the scopes selected to be displayed (Figure 25) present a good overview of the current system design and allow, in particular, BER estimation directly from the eye diagram traces.

7. Concluding Observations

In this report we have considered the three main components which form a simple, yet typical single channel optical fiber communication link including the transmitter, optical fibers –standard and compensating types and receiver. To our knowledge this optical DQPSK simulator is the first to have been reported and developed in the Matlab™ Simulink platform. The flexible nature of Simulink and its wide range of pre-designed block sets allow several important features for implementation of optically amplified transmission systems.

Although the development of the Simulator in the Simulink platform can be time consuming, gaining an understanding of the physical carrier phases of the DQPSK system is considered as the most challenging tasks. It has been found that the DQPSK modulation format can and has been implemented in different ways using alternative hardware ranging from integrated lasers and dual drive Mach-Zehnder modulator devices to simple configurations using MZIM's and PM's.

We have stated that the DQPSK modulation format offers twice the bandwidth compared to conventional OOK. Apart from the di- bit coding aspect of this modulation format and the increase in spectral efficiency (b/s/Hz) that would be observed in DWDM systems, presentation of results that prove the superiority (to OOK) of this format. In this simulator we have modeled for the detection case using a single PD.

Apart from the di- bit coding aspect of this modulation format and the increase in spectral efficiency (b/s/Hz) that would be observed in DWDM systems, presentation of results that prove the superiority (to OOK) of this format. In this simulator we have modeled for the detection case using a single PD. Balanced detection or receiver diversity would significantly improve the BER performance by at least 3.5 dB. We have also included the eye diagram results for 10 GB/s RZ-OOK from the MOCSS 2000 optical simulator, updated recently for comparison and for completeness.

Regarding the fiber propagation model, we have not implemented in this part but reserved for Part V, the fiber split step Fourier model. However the linear fiber model as a low pass filter is proved to present sufficiently accurate on dispersion effects provided the total optical power is below the nonlinear SPM threshold.

The simplicity to develop in the Simulink environment is also a positive factor. Due to the good linkage developed between all parts of the series the 10 GB/s DWDM optical fiber systems, the optimization of various block components are achieved. The development of the simulator for 10Gb/s and 40Gb/s single channel DQPSK has been proposed to provide, unlike other commercial packages such as VPI Systems, the most effective and simplified simulation. This simulator has, as required, simulated the most complex modulation format of the family of optical modulation techniques proposed in literature of digital optical band.

It is thus now possible to remove the limitations of hardware and extend to the signaling Aspects to improve transmission capacity. We have demonstrated a 20Gbps (2 X 10Gbps) single channel optical DQPSK simulator which is capable of doubling the bit rate compared to conventional OOK signaling techniques.

The simulator has been developed in the Matlab subsidiary program simulink and due to its nature can easily be altered to suite the user specifications or to improve system optimization. All-optical components necessary to transmit, propagate and decode/ receive the transmitted bit stream have been implemented in the simulator along including the superposition of added noises etc.

Transmitter components include the MZIM and PM along with the optical carrier and electrical bit stream PRBS generators. The fiber has been developed using a linear LPF model which only takes into account the linear dispersion effects of optical fibers. We have shown that without appropriate dispersion management, the phase information coded in adjacent symbols is corrupted.

We have also demonstrated that the simulator is a good tool for altering system specifications such as dispersion factors of fiber and providing quick results for performance comparisons. The simulator is extended in the future to simulate dense and super-dense WDM long-haul transmission systems. This work has provided the framework for individual channels that would compose the DWDM system. Given that we have successfully demonstrated 20Gbps transmission using a single DQPSK channel with a BER of 10-12 an extension to the T bps would become a possibility.

Screen shot for our simulator:

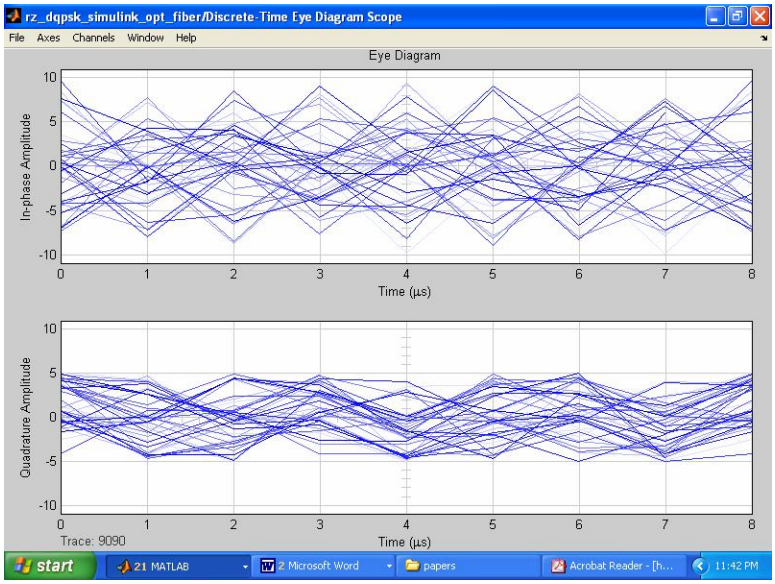

Fig25: Eye Diagram which represent BER.l

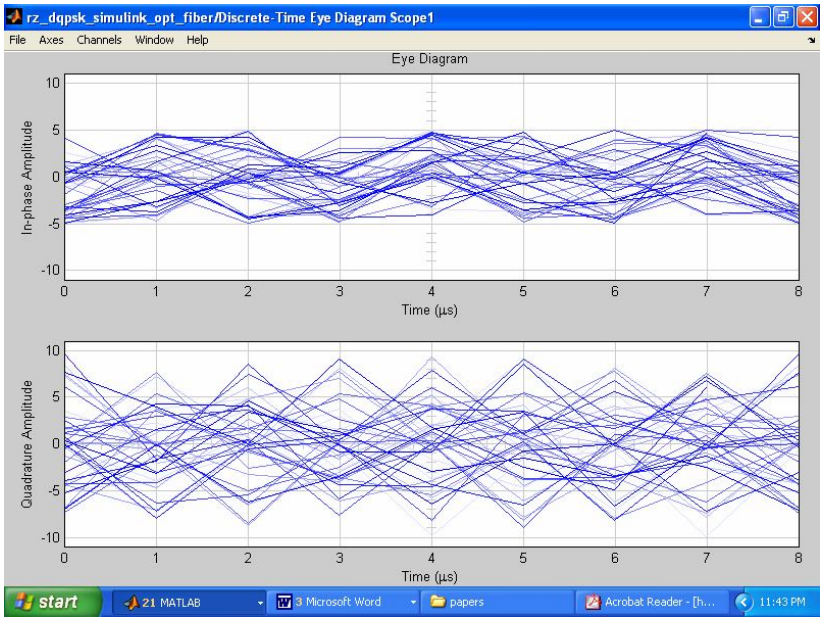

Fig26: Eye Diagram which represent BER.2

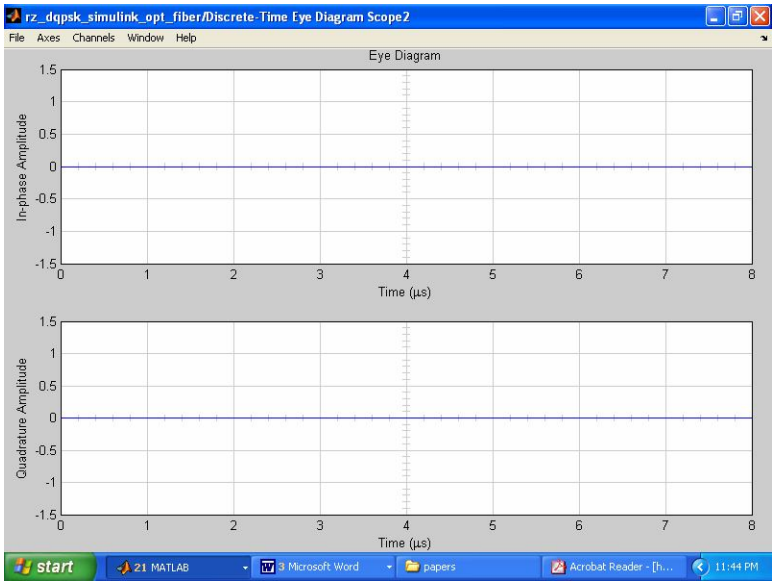

Fig27: Eye Diagram which represent without BER.3

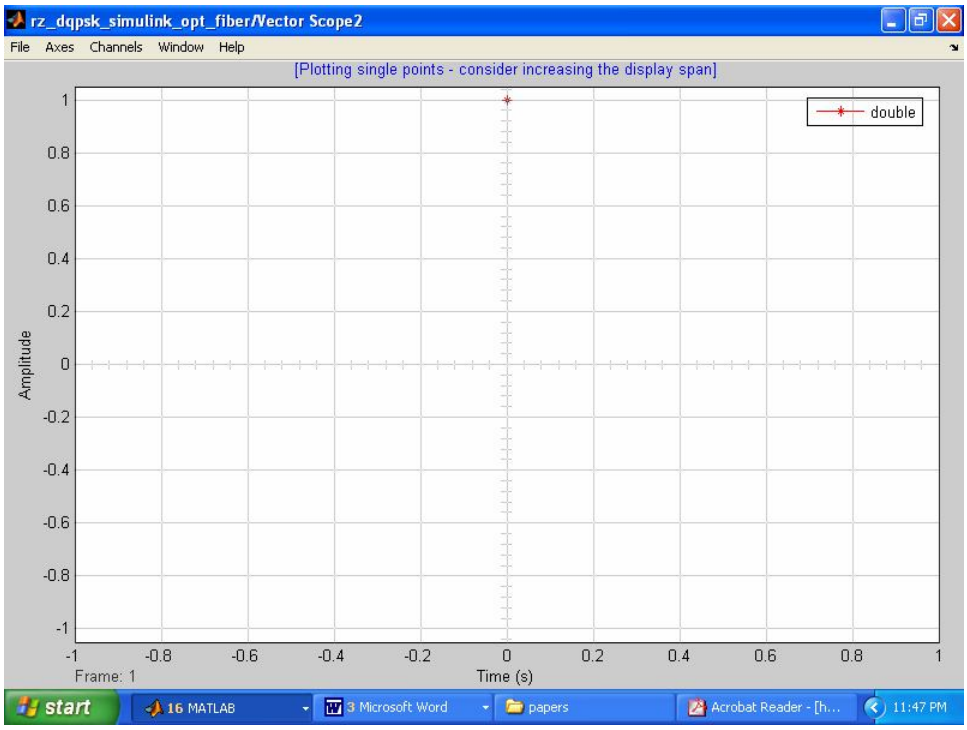

Fig 28: Output for Vector scope with horizontal point.

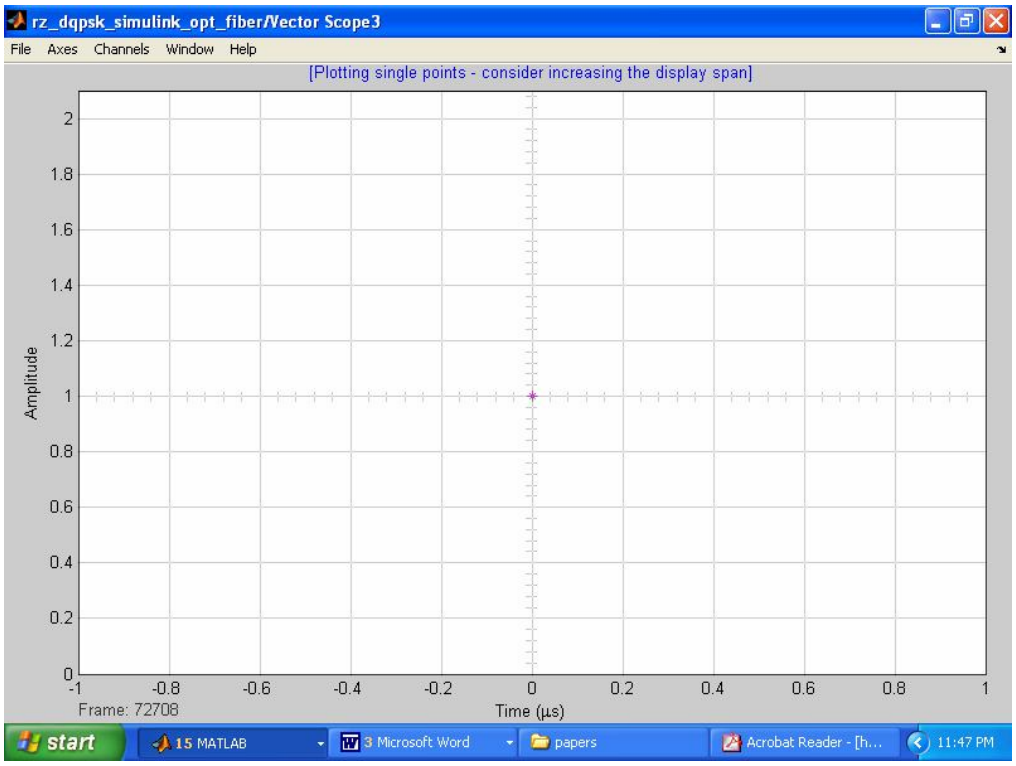

Fig 29: Output for Vector scope with Center point. (di-bit)

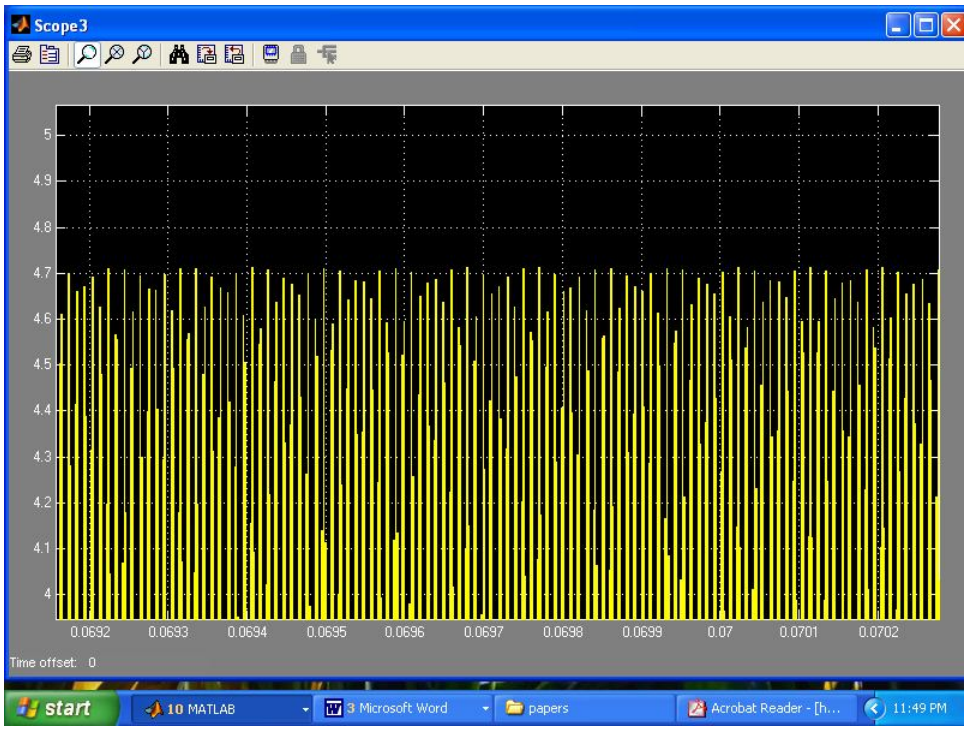

Fig-30: Scope out put1.

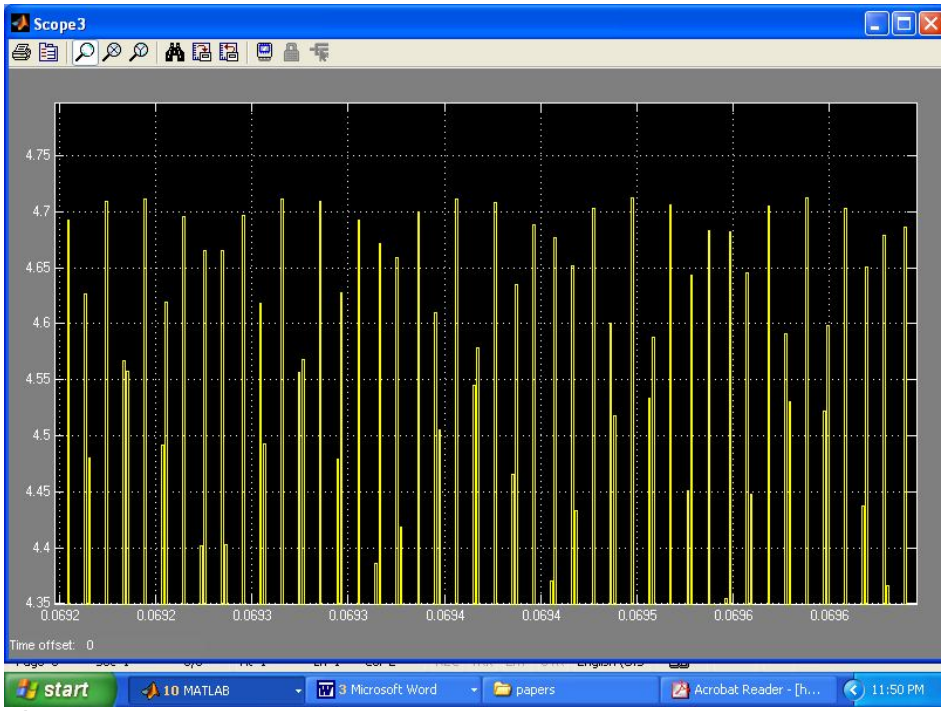

Fig-31: Scope out put2.

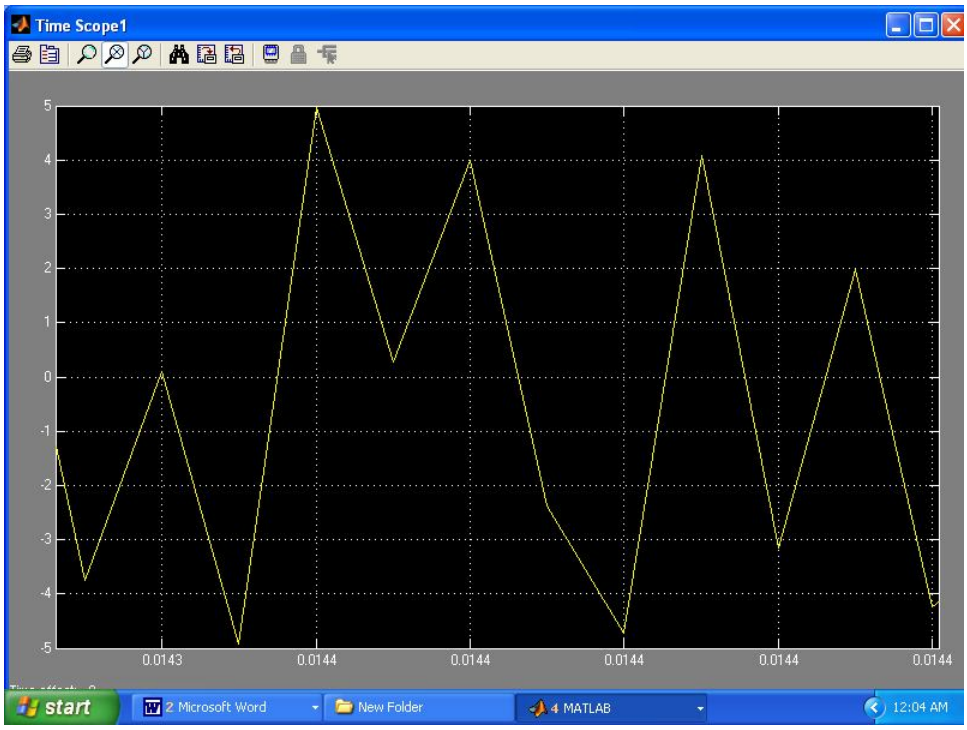

Fig 32: Input signal showed in time scope

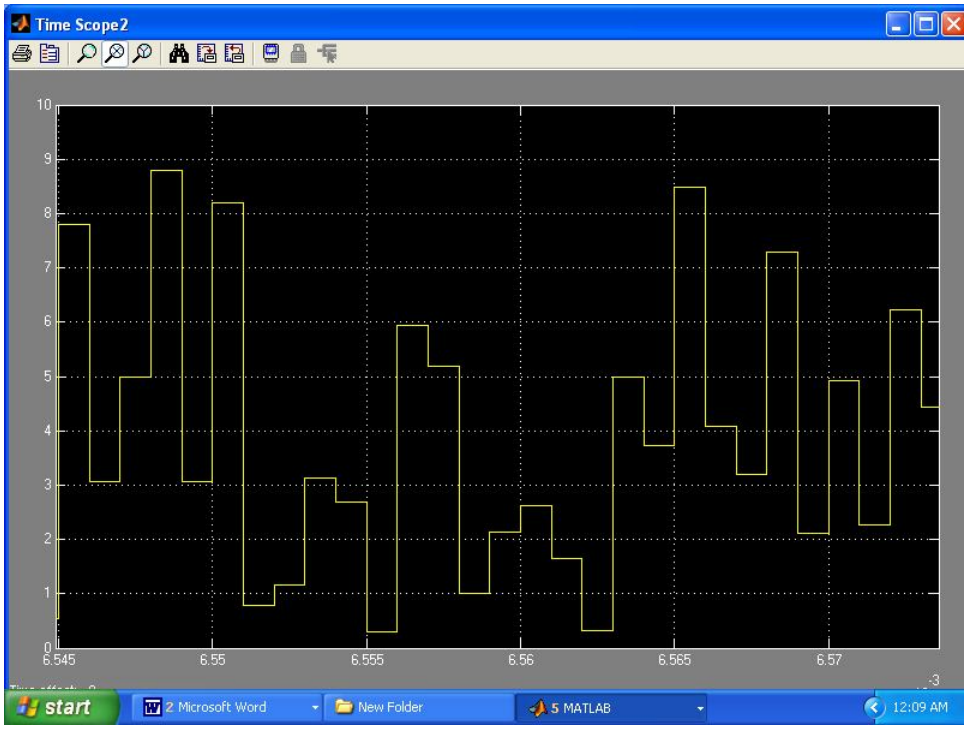

Fig 33: Input signal showed in time scope 2

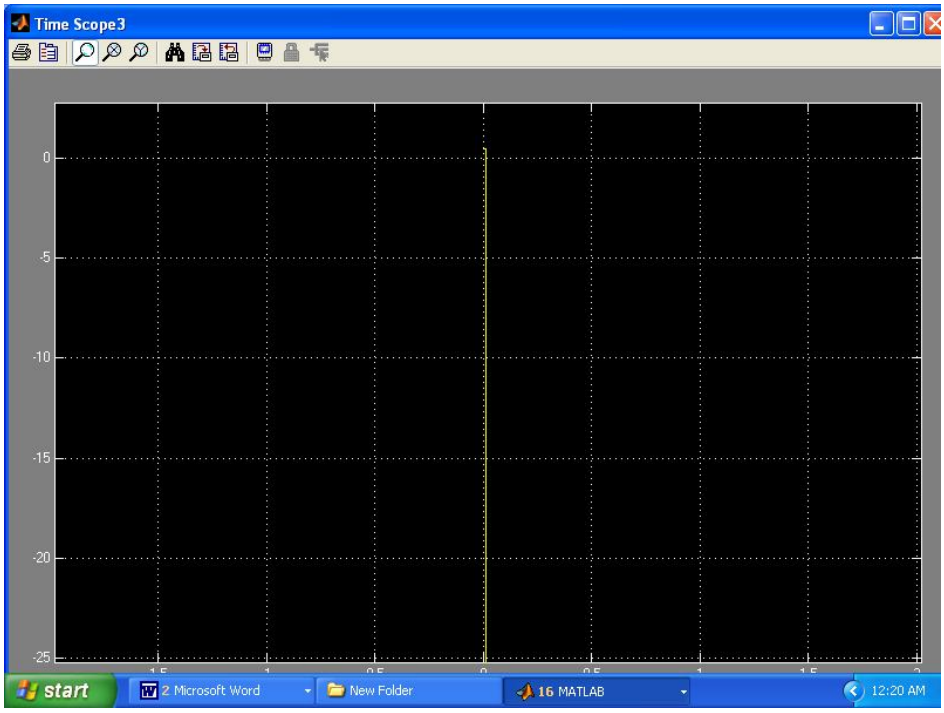

Fig 34: ignal showed in time scope 3 which represent output of the channel.

8. REFERENCES

[1] L. N. Binh, Lam,D., Chi, K.Y., "Monash Optical Communications Systems Simulator," ECSE Monash University, Melbourne Australia 1997.

[2] L. N. Binh, and Li, C.H.,, "EDFA Simulink Simulator," Monash university, MelbourneAustralia 2004.

[3] B. Zhu, ""3.08 Tbit/s (77 ´ 42.7 Gbit/s) WDM transmission over 1200 km fibre with 100 km repeater spacing using dual C- and L-band hybrid Raman/erbium-doped inline amplifiers"," *Elect. Lett*, vol. 37, 2001, 21 June.

[4] E. Yamada, " "106 channel 10 Gbit/s, 640 km DWDM transmission with 25 GHz spacing with supercontinuum multi-carrier source"," *Elect. Lett.*,, vol. 37, 2001.

[5] C. Wree, " "RZ-DQPSK format with high spectral efficiency and high robustness towards fiber nonlinearities"," University of Kiel, 2002.

[6] A. Carena, "'A time domain optical transmission system simulation package accounting for Nonlinear and Polarization-related effects in fiber'; ." *IEEE J. Selected Areas in Communications*, vol. 15, 1997.

[7] M. J. N. Sibley, *Optical components and systems*, 2nd ed: J.Wiley, 1995.

[8] L. N. Binh, *ECE 4405 Lecture Notes on Optical Communications Systems*. Melbourne, Australia: MiTec, 2003

[9] J. T. Gallo, " 'Optical Modulators for fiber systems';," presented at IEEE GaAs Digest;p. 145, 2003.

[10] A. F. Elrefaie, "Chromatic Dispersion limitations in coherent lightwave transmission systems';," *IEEE J. Lightwave Technology*, vol. 6, 1988, May.

[11] Corning, *Corning :Fiber-Optic Technology Tutorial; The International Engineering Consortium*.

[12] L. N. Binh, ""An introduction to optical planar waveguides and optical fibers";," Department of Electrical and Computer systems engineering; Monash University, 1997, pp. 20-21.

[13] S. V. Kartalopoulos, *"Introduction to DWDM technology: Data in a rainbow"*: J Wiley, 2001.

[14] K.-P. Ho, "Raised Cosine function in time domain as defined "Spectrum externally modulated optical signals," *IEEE J. Lighjtw. Tech.*, 2004.

[15] H. Kim, " H. Kim "Robustness to Laser Frequency Offset in Direct-Detection DPSK and DQPSK systems"," *IEEE J. Lightwave Technology*,, vol. 21, 2000.

[16] a. W. Gnauck A.H., P.J., " "Tutorial on Phase-Shift-Keyed Transmission"," presented at OFC 2004, 2004.

[17] S. E. Miller, *"Optical Fiber Communication 2";*: Academic Press, 1988.

[18] C. Wree, " "Experimental Investigation of receiver sensitivity of RZ-DQPSK modulation format using balanced detection";," presented at OFC2003, 2003.

[19] P. E. Green, *"Fiber Optic Networks"*: Prentice Hall, 1993.

[20] J. G. Proakis, *Digital Communications*, 3rd ed. New York: McGraw-Hill, 1995.

[21] J. C. Palais, *"Fiber Optic Communications"*: Prentic Hall, 1984.

[22] J. Armstrong, ""Simulink Optical Simulator"," in *Electrical and Computer Systems Engineering*. Clayton, Australia: Monash, 2003, pp. 62.

[23] A. Carera, " 'A time domain optical transmission system simulation package accounting for Nonlinear and Polarization-related effects in fiber' I.," *IEEE J. Selected Areas in Communications*, vol. 15, 1997.

[24] A. E. Elrefaie, " 'Chromatic Dispersion limitations in coherent lightwave transmission systems'," *IEEE J. Lightwave Technology*, vol. 6, 1988.

[25] G. P. Agrawal *Fiber-optic Communication Systems*, 2nd ed. N.Y.: Academic Press, 2002.

[26] G. Keiser, *"Optical Fiber Communication*. New York: McGraw Hill, 1991.

[27] X. Wei, " 'Numerical Simulation of the SPM penalty in a 10Gb/s RZ-DPSK system'," *IEEE Photonics technology Letters*, vol. 15, 2003.

[28] L. N. Binh, *"Optical Receiver: Noise and Sensitivity considerations for OFCS and networks"*. Melbourne Australia: MiTec, 2003.

[29] *Investigations of high bit rate optical transmission systems employing a channel data rate of 40 Gb/s.*,by Anes hodzi and aus Berlin, July 2004.

[30] G. Bosco, A. Carena, V. Curri, R. Gaudino, and P. Poggiolini. *On the use of NRZ, RZ and CSRZ modulation formats for ultra-dense WDM at 40 Gb/s*. European Conference on Optical Communication (ECOC), 3(P3.7), September 2002.

[31] A. Hodzic, B. Konrad, S. Randel, and K. Petermann. *Optimized filtering for 40-Gb/s/channel-based DWDM transmission systems over standard single mode fiber*. IEEE Photonics Technology Letters, July 2003.

[32] G. Lenz, B. J. Eggleton, C. K. Madson, C. R. Giles, and G. Nykolak. *Optimal dispersion of optical filters for WDM systems*. IEEE Photonics Technology Letters, 10(4):567–569, April 1998.

[33] K. Petermann. *Laser Diode Modulation and Noise. Kluwer Academics* Publishers, 1988.

A List of symbols

B Acronyms

RZ Return-to-Zero
ASE Amplified Spontaneous Emission
AWG Arrayed Waveguide Grating
al-CNRZ Alternate Chirped Non-Return-to-Zero
al-PNRZ Alternate Polarized Non Return-to-Zero
al-PRZ Alternate Polarized Return-to-Zero
BER Bit Error Rate
CRZ Chirped Return-to-Zero
CSRZ Carrier Suppressed Return-to-Zero
DCF Dispersion Compensating Fiber
DCS-RZ Duobinary Carrier Suppressed Return-to-Zero
DD Direct Detection
DFB Distributed Feedback
DGD Differential Group Delay
DQPSK Differential Quadrature Phase Shift Keying
DPSK Differential Phase Shift Keying
DR Dynamic Range
DRZ Duobinary Return-to-Zero
DMUX Demultiplexer
DSF Dispersion Shifted Fiber
DSL Digital Subscriber Line
DWDM Dense Wavelength Division Multiplexing
EAM Electro Absorption Modulator
EDFA Erbium Doped Fiber Amplifier
ETDM Electrical Time Division Multiplexing
FFT Fast Fourier Transformation
FKE Franz Kaldysh E_ect
FM Frequency Modulation
FSK Frequency Shift Keying
FWM Four Wave Mixing
GD Group Delay
GVD Group Velocity Dispersion
IP Internet Protokol
IM Intensity Modulation
IM-DD Intensity Modulation Direct Detection
ISI Inter Symbol Interference
ITU International Telecommunication Union
IXPM Intrachannel Cross Phase Modulation
LPF Low Pass Filter

MAN Metro Area Netweork
MSK Minimum Shift Keying
MUX Multiplexer
MZI Mach Zehnder Interferometer
MZM Mach Zehnder Modulator
NF Noise Figure
NRZ Non Return-to-Zero
OSNR Optical Signal-to-Noise Ratio
OSI Open System Interconnection
OXC Optical Cross Connect
QoS Quality of Service
PLL Phase Locked Loop
PM Phase Modulator
PMD Polarization Mode Dispersion
PMF Polarization Maintaining Fiber
PSD Power Spectral Density
PSK Phase Shift Keying
RZ Return-to-Zero
SOA Semiconductor Optical Amplifier
SPM Self Phase Modulation
SSB-RZ Single Side Band Return-to-Zero
SSFM Split Step Fourier Method
SSMF Standard Single Mode Fiber
WDM Wavelength Division Multiplexing
XPM Cross Phase Modulation

Waveforms used for communication

The most popular optical bit streams are NRZ and RZ formats. NRZ format is Non-Return-to-Zero, in which “1”s are represented by one level and “0”s are represented by the other level. The pulse remains on throughout the bit slot and the amplitude never drops to zero. Pulse width has a direct relation with this representation. Clock recovery is usually more difficult with NRZ coding because loss of timing would occur if there are long strings of the same amplitude level.

This can be overcome by the use of block codes and scrambling. NRZ uses the full bit duration while transmission. Since the pulse width has a direct relationship with the representation, it may lead to bit-pattern-dependent effects if the optical pulse spreads during transmission .Also NRZ uses smaller signal bandwidth.

RZ format has attracted a lot of attention to satisfy the needs of higher data rates. In this format, the “1” bit is shorter than the bit interval, the amplitude returns to zero and typically occupying 50% of the bit slot and the “0” bit always stays at amplitude level “0”. A long string of “0” can cause de-synchronization. This can be overcome by using a bi-phase or optical Manchester code. Twice the bandwidth of NRZ coding is required due to the usage of half the bit duration for data transmission resulting in Increased capacity.

Modulation technique

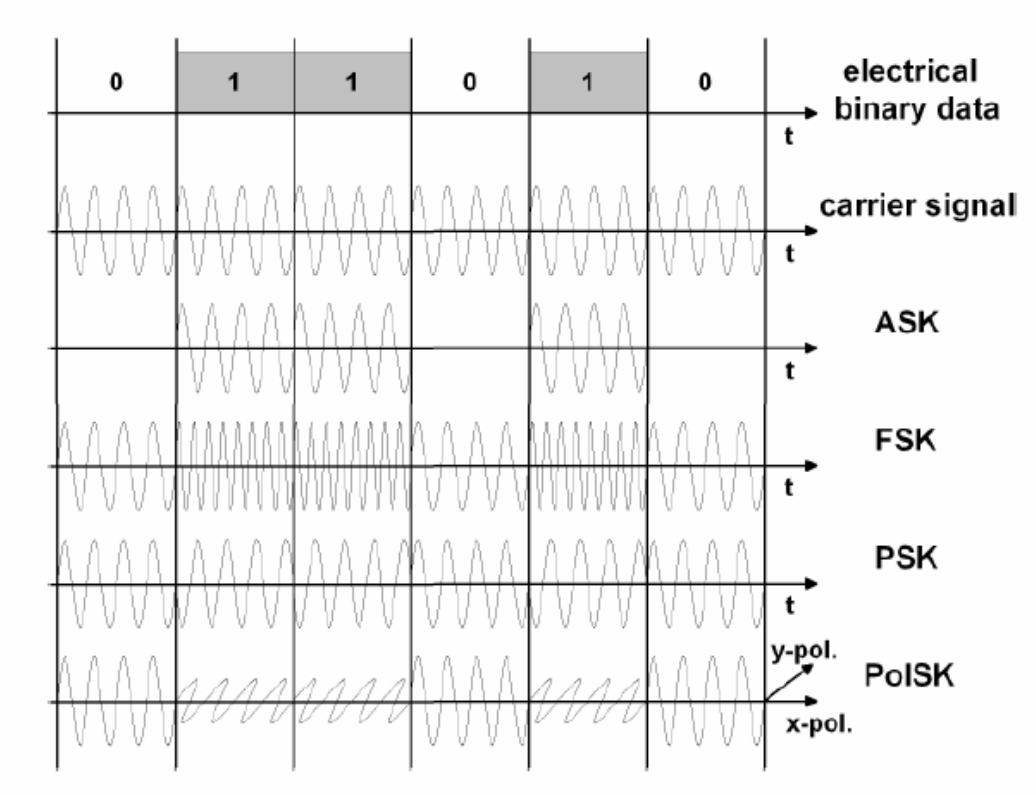

Fig 35: Modulation formate.

END